The Journal of Neuroscience, July 15, 2000, 20(14):5401–5419

Selective Alterations in $GABA_A$ Receptor Subtypes in Human Temporal Lobe Epilepsy

Fabienne Loup,[1] Heinz-Gregor Wieser,[2] Yasuhiro Yonekawa,[3] Adriano Aguzzi,[4] and Jean-Marc Fritschy[1]

[1]Institute of Pharmacology, University of Zurich, and Departments of [2]Neurology, [3]Neurosurgery, and [4]Neuropathology, University Hospital Zurich, 8057 Zurich, Switzerland

Temporal lobe epilepsy (TLE) is associated with impaired inhibitory neurotransmission. Studies in animal models suggest that $GABA_A$ receptor dysfunction contributes to epileptogenesis. To understand the mechanisms underlying TLE in humans, it is fundamental to determine whether and how $GABA_A$ receptor subtypes are altered. Furthermore, identifying novel receptor targets is a prerequisite for developing selective antiepileptic drugs. We have therefore analyzed subunit composition and distribution of the three major $GABA_A$ receptor subtypes immunohistochemically with subunit-specific antibodies (α1, α2, α3, β2,3, and γ2) in surgical specimens from TLE patients with hippocampal sclerosis ($n = 16$). Profound alterations in $GABA_A$ receptor subtype expression were observed when compared with control hippocampi ($n = 10$). Although decreased $GABA_A$ receptor subunit staining, reflecting cell loss, was observed in CA1, CA3, and hilus, the distinct neuron-specific expression pattern of the α-subunit variants observed in controls was markedly changed in surviving neurons. In granule cells, prominent upregulation mainly of the α2-subunit was seen on somata and apical dendrites with reduced labeling on basal dendrites. In CA2, differential rearrangement of all three α-subunits occurred. Moreover, there was layer-specific loss of α1-subunit-immunoreactive interneurons in hippocampus proper, whereas surviving interneurons exhibited extensive changes in dendritic morphology. Throughout, expression patterns of β2,3- and γ2-subunits largely followed those of α-subunit variants. These results demonstrate unique subtype-specific expression of $GABA_A$ receptors in human hippocampus. The significant reorganization of distinct receptor subtypes in surviving hippocampal neurons of TLE patients with hippocampal sclerosis underlines the potential for synaptic plasticity in the human GABA system.

Key words: human epilepsy; $GABA_A$ receptor; dentate gyrus; hilus; CA2; pyramidal cells; granule cells; interneurons

Fast synaptic inhibition in the vertebrate CNS is mediated primarily by the neurotransmitter GABA interacting with the $GABA_A$ class of receptors. Impaired GABA transmission can lead to neuronal hyperexcitability, a condition associated with epileptogenesis. Furthermore, antiepileptic agents that enhance $GABA_A$ receptor function are effective in treating seizures (Olsen et al., 1999).

Temporal lobe epilepsy (TLE) is the most common adult seizure disorder and, when associated with hippocampal sclerosis (HS), is the most refractory to pharmacotherapy (Engel, 1998; Semah et al., 1998). Evidence from human studies suggests that postsynaptic $GABA_A$ receptors contribute to the pathophysiology of TLE with HS. Thus, alterations in $GABA_A$ receptor function and in their allosteric modulation by ligands of the benzodiazepine-binding site were documented in hippocampal neurons from HS patients (Franck et al., 1995; Williamson et al., 1995, 1999; Isokawa, 1996; Shumate et al., 1998; Brooks-Kayal et al., 1999). Furthermore, *in vivo* imaging and autoradiographic studies demonstrated a decrease in central benzodiazepine receptor binding primarily attributed to extensive cell death in the sclerotic hippocampus of TLE patients (Olsen et al., 1992; Burdette et al., 1995; Koepp et al., 1996) and additional reduction of receptor density per remaining neuron in CA1 (Johnson et al., 1992; Hand et al., 1997; Koepp et al., 1998).

The recognition of multiple $GABA_A$ receptor subtypes and their differential expression in distinct neuronal populations (Fritschy and Möhler, 1995; McKernan and Whiting, 1996; Sperk et al., 1997) permits a target-oriented analysis of $GABA_A$ receptor dysfunction in human TLE. $GABA_A$ receptor heterogeneity results from the combinatorial assembly of a multitude of subunit variants encoded by at least 20 genes (α1–6, β1–4, γ1–3, δ, ϵ, π, θ, and ρ1–3) (Möhler et al., 1996; Barnard et al., 1998; Whiting et al., 1999). If expression of specific $GABA_A$ receptor subtypes is altered in TLE, their identification would facilitate the development of more selective antiepileptic drugs and ligands for *in vivo* imaging. Current approaches, however, have not provided the degree of spatial resolution and specificity required to characterize individual receptor subtypes and their subunit-specific alterations in human brain. Although recent studies in animal models of TLE reported changes in the number and subunit composition of $GABA_A$ receptors in hippocampal neurons (Schwarzer et al., 1997; Brooks-Kayal et al., 1998; Nusser et al., 1998; Bouilleret et al., 2000), the validity of these data as pertains to human TLE remains to be established.

In the present study, we investigated alterations in subunit architecture and localization of $GABA_A$ receptor subtypes in hippocampi resected from TLE patients with HS and compared these with control tissue obtained at autopsy and with specimens from TLE patients without HS. A protocol based on microwave irradiation and tyramide signal amplification was used to visualize the major $GABA_A$ receptor subunits α1, α2, α3, β2,3, and γ2 in human brain tissue using subunit-specific antisera (Loup et al., 1998).

Parts of this paper have been published previously as abstracts (Loup et al., 1997, 1999).

MATERIALS AND METHODS

Patient selection. Twenty-one patients (mean age, 34.9 ± 2.5 years; range, 15–56 years) undergoing surgery for medically intractable TLE were included in this study. All procedures were performed with consent of the patients and were approved by the Ethics Committee of the University Hospital Zurich in accordance with the Helsinki Declaration of 1975. Presurgical assessment consisted of detailed history and neurological examination, semi-invasive EEG monitoring with foramen ovale electrodes, and neuropsychological testing. Neuroradiological studies included for all cases high-resolution magnetic resonance imaging (MRI) with special protocols to visualize the hippocampal formation and positron emission tomography (PET) with ^{18}fluoro-2-deoxyglucose. Intraoperative electrocorticography was performed in all subjects to further characterize the

Received March 14, 2000; revised May 3, 2000; accepted May 3, 2000.

This work was supported by the Théodore OTT Fund (F.L.) and Swiss National Science Foundation Grant 31–52869.97 (J.M.F.). We are grateful to Prof. Hanns Möhler for his continuous support and we thank Dr. Florence Crestani for advice on statistics and Dr. Urs Gerber for comments on this manuscript.

Correspondence should be addressed to Dr. Fabienne Loup, Institute of Pharmacology, University of Zurich, Winterthurerstrasse 190, CH-8057 Zurich, Switzerland. E-mail: loupf@pharma.unizh.ch

epileptogenic zone to be resected. Based on clinical, EEG, neuroimaging, and neuropathological data, patients were classified into those with HS ($n = 16$; mean age, 36.9 ± 2.7 years; range, 17–56 years) and those without HS (non-HS; $n = 5$; mean age, 28.2 ± 5.6 years; range, 15–44 years) (Wieser et al., 1993). Patients from the HS group underwent selective amygdalohippocampectomy consisting in resection of amygdala, hippocampal formation, and parahippocampal gyrus (Wieser and Yasargil, 1982). The HS group included patients with severe damage to the hippocampus as assessed by MRI and PET studies, with the epileptogenic focus localized to the mesial temporal region, and, in most cases, with a history of seizures from childhood. The origin of TLE in the non-HS patients was attributed to a tumor ($n = 3$) or vascular malformation ($n = 1$) identified by neuroimaging in an extrahippocampal location and confirmed histopathologically, and in one case no lesion was apparent. In these patients, the surgical procedure consisted of amygdalohippocampectomy alone or with resection of the epileptogenic lesion or part of temporal lobe. For comparison, hippocampi from five subjects (mean age, 58 ± 6.2 years; range, 40–73 years) with no history of neurological or psychiatric disorder were collected at autopsy between 8 and 16 hr after death (mean postmortem interval, 11.2 ± 1.3 hr). Hippocampal tissue was also obtained from a 56-yr-old patient with known TLE and HS with a postmortem interval of 15 hr, who had died from multiorgan failure.

Tissue preparation. Hippocampal specimens obtained at surgery or autopsy were cut into 7- to 12-mm-thick blocks transversely to the long axis. In surgical TLE cases, the rostrocaudal extent of the hippocampus available for study ranged from 7.2 to 17.6 mm for HS specimens (mean length, 12.6 ± 0.75 mm) and from 8 to 12 mm for non-HS specimens (mean length, 9.6 ± 0.72 mm). For all specimens, the sampled part of hippocampus comprised rostral and middle levels. When tissue was obtained at autopsy, the whole hippocampus was collected. After rinsing in PBS at pH 7.4 immediately on resection in the operating room or after dissection at autopsy, tissue blocks were immersion-fixed for 6–8 hr at 4°C under constant agitation in a mixture of 4% freshly dissolved paraformaldehyde and 15% saturated picric acid in 0.15 M phosphate buffer at pH 7.4 (Somogyi and Takagi, 1982). After fixation, tissue blocks were pretreated using a modified antigen-retrieval method based on microwave irradiation as described previously (Fritschy et al., 1998) and adapted to human tissue (for details, see Loup et al., 1998). Tissue blocks were cryoprotected in 10, 20, and 30% sucrose in PBS over a period of 3–4 d, frozen at −28°C in isopentane, and stored at −80°C. Subsequently, series of 40-μm-thick sections were cut in a cryostat and collected in ice-cold PBS. They were then either processed for immunohistochemistry (see below) or transferred to antifreeze solution [50 mM phosphate buffer, 15% sucrose, 30% (v/v) ethylene glycol, and sodium azide, pH 7.4] and stored at −20°C until use. This procedure allowed 10–12 different specimens, including tissue from autopsies, to be processed in parallel during the same session. Staining for the $GABA_A$ receptor subunits was performed on consecutive sections (five series), and the space between sections from one series was between 720 and 800 μm. An additional adjacent series of sections was Nissl-stained for histopathological examination.

Immunohistochemistry. The following subunit-specific antibodies were used: mouse monoclonal antibodies bd-24 and bd-17 recognizing the human $GABA_A$ receptor α1-subunit and both the β2- and β3-subunits, respectively (Schoch et al., 1985; Ewert et al., 1990), and polyclonal guinea pig antisera recognizing the α2-, α3- and γ2-subunits (Loup et al., 1998). The preparation and characterization of the polyclonal antibodies, raised against synthetic peptides derived from rat cDNA sequences, have been described (for details, see Fritschy and Möhler, 1995). For each subunit, the amino acid sequences used as antigens were found to be identical in rat and human cDNAs, and the high specificity of the $GABA_A$ receptor subunit antibodies in human brain tissue was verified with Western blot analysis (Waldvogel et al., 1999). Free-floating sections were preincubated in 1.5% H_2O_2 in PBS for 10 min at room temperature to block endogenous peroxidase activity. They were then washed three times for 10 min in PBS and processed for immunoperoxidase staining (Hsu et al., 1981) as described previously (Loup et al., 1998). The dilutions of the antibodies were: α1-subunit (monoclonal antibody bd-24), 0.2 μg/ml; α2-subunit (affinity-purified), 1.3 μg/ml; α3-subunit (affinity-purified), 1.8 μg/ml; β2,3-subunit (monoclonal antibody bd-17), 3.8 μg/ml; and γ2-subunit (crude serum), 1:1500. Control experiments for staining specificity included the replacement of primary antibodies with nonimmune serum and preadsorption of the antibodies with 3–5 μg/ml of their respective peptide antigen (Fritschy and Möhler, 1995; Loup et al., 1998). No specific staining was seen in either case. To assess the subcellular localization of $GABA_A$ receptor subunits in individual neurons with confocal laser-scanning microscopy, immunofluorescence staining with tyramide signal amplification (TSA kit; NEN Life Science Products, Brüssels, Belgium) was performed (Loup et al., 1998).

Data analysis. Sections were analyzed with a Zeiss (Jena, Germany) Axioplan microscope equipped for bright-field and epifluorescence microscopy. Photomicrographs were taken with Eastman Kodak (Rochester, NY) T-max 100 film. Sections processed for immunofluorescence staining were also analyzed by confocal laser-scanning microscopy (TCS 4D; Leica, Heidelberg, Germany) using Imaris software (Bitplane, Zurich, Switzerland) for image processing.

Nomenclature. The nomenclature of Lorente de Nó (1934) was used except for the hilar region where the classification proposed by Amaral (1978) and later described for the human hippocampus was adopted (Amaral and Insausti, 1990). Accordingly, the portion of the pyramidal layer that inserts into the dentate hilus (CA3c and/or CA4 in the terminology of Lorente de Nó, 1934) is referred to as CA3.

Neuron counts. Nissl-stained sections from all specimens were examined to assess the presence of pathological alterations in general and the degree of hippocampal sclerosis in epileptic samples in particular. In addition, neurons were counted in the regions where densitometric measurements of $GABA_A$ receptor subunit staining intensity were obtained, using immediately adjacent Nissl-stained sections from autopsy ($n = 5$), non-HS ($n = 5$), and HS cases ($n = 16$). Nucleolar profiles of CA2 pyramidal cells and nuclear profiles of granule cells were counted within a 12.5 × 12.5 mm ocular grid consisting of 10 × 10 squares at a magnification of 400 and 1000×, respectively. Four to six measurements per region and section were averaged where all nuclei visible in the section were counted except for those touching the top and right edges of the grid. Typically, in autopsy and non-HS cases, the width of the granule cell layer was included in a single counted field (125 × 125 μm area), whereas in HS cases with granule cell dispersion, two or sometimes three fields were necessary to include all granule cells. To account for this factor, granule cells were also counted within a 125-μm-wide column through the granule cell and molecular layers (Houser, 1990). Moreover, in some HS cases, granule cells displayed elongated cell bodies that appeared larger. Therefore, no assumption-based methods were used, and the results were expressed as mean number of neuronal profiles per square millimeter and additionally, for granule cells, per column. The counts were not performed in a stereological manner, because the intention was to represent the distribution of these neurons in relative terms suited for intergroup comparison and that such procedures are not amenable to surgically collected tissue where random sampling is difficult and tissue volume changes caused by hippocampal sclerosis cannot be estimated.

The numbers of interneurons immunoreactive for the α1-subunit were assessed in the CA2 and CA3 areas using the grid procedure described above. Counts were done at a magnification of 200× in strata pyramidale, radiatum, and lacunosum-moleculare, and additionally for CA3, in stratum lucidum. While strata pyramidale, lacunosum-moleculare, and lucidum did not show signs of major atrophy in HS cases as measured by their respective widths, stratum radiatum had undergone variable and at times severe reduction. For this reason and because the borders between strata were readily delimited, counts were obtained within an area consisting of 625 μm × the thickness of the stratum where the cells were counted. Two to three counts per stratum and region were made in two sections from each specimen. In a few surgical cases, mostly non-HS, it was not possible to obtain α1-subunit-positive interneuron counts in certain CA2 or CA3 strata because of damage during the resection procedure.

Densitometric measurements. Sets of six adjacent sections were considered for each case analyzed: one Nissl-stained and five immunostained sections. The intensity of labeling for the $GABA_A$ receptor subunits α1, α2, α3, β2,3, and γ2 was measured by densitometry in sections from autopsy ($n = 5$), non-HS ($n = 3$), and HS cases ($n = 14$) at equivalent midrostrocaudal levels of the hippocampus. Sections were imaged using a high-resolution video camera (1280 × 1024 pixels) interfaced with a Zeiss microscope under a 10× objective. Before conducting the measurements, the computer-assisted imaging device MCID M5 (Imaging Research, St. Catherines, Ontario, Canada) was calibrated with a set of neutral density filters (Eastman Kodak) to automatically convert gray levels to optical density values. Illumination and filter settings were maintained at the same level for image acquisition and densitometric analysis for all specimens. Optical density (OD) measurements were recorded in the CA2 area and the dentate gyrus. For CA2 analysis, two rectangles with an area of 68,600 μm^2 each were used to measure the average OD per section in the pyramidal cell layer. In the dentate gyrus, the average OD was calculated from measurements in five circles with an area of 1020 μm^2 each in the granule cell layer, the inner molecular layer, the outer molecular layer, and the subgranular layer in both the upper and lower blades. Because the epileptic samples contained no region where staining for one or more of the $GABA_A$ receptor subunits was judged to be unequivocally unaffected, the results were not normalized to a reference value. Variability was greatly minimized, however, by the highly standardized tissue preparation protocol and the immunohistochemical processing in parallel of 10–12 different samples from autopsy, non-HS, and HS cases.

Statistical analysis. Neuron counts and densitometric measurements were analyzed for statistical significance using the Kruskal–Wallis test (nonparametric ANOVA; InStat program). Data were further compared between individual groups (at $p < 0.05$) with a multiple comparisons test.

RESULTS

Patient history

Medical records from all seizure patients were reviewed for relevant clinical parameters. Whereas no significant difference was found for the age at surgery (HS group: 36.9 ± 2.7 years, range, 17–56 years, $n = 16$; non-HS group: 28.2 ± 5.6 years, range, 15–44 years, $n = 5$), seizures had lasted longer and usually started earlier in HS patients compared with non-HS patients (duration of the

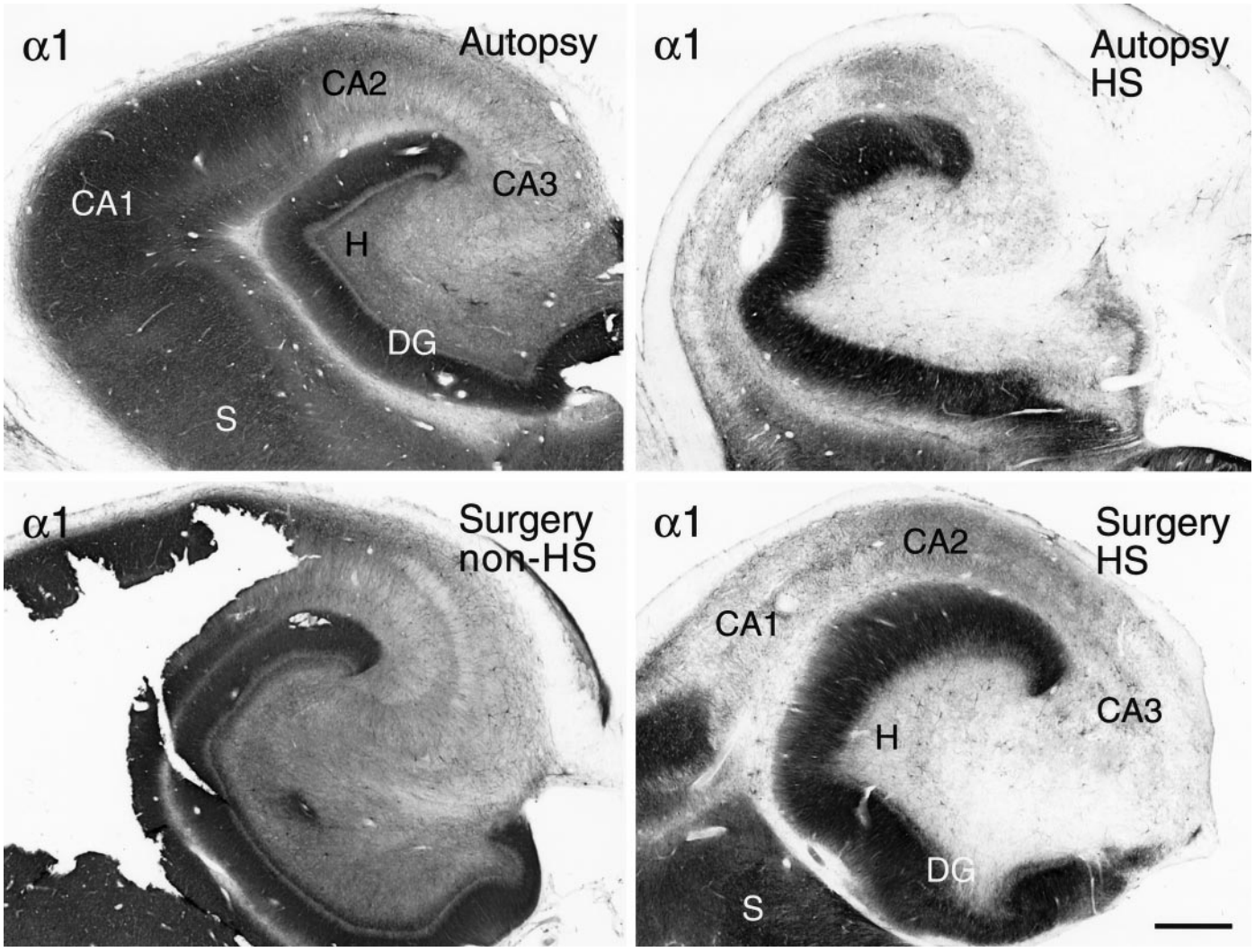

Figure 1. Validation of controls. Hippocampal tissue obtained at autopsy does not differ from hippocampal tissue removed surgically with respect to $GABA_A$ receptor immunoreactivity. These examples show α1-subunit staining: autopsy control, without neurological disease (*top left*), surgical control, TLE without HS (*bottom left*), autopsy, TLE with HS (*top right*), and surgery, TLE with HS (*bottom right*). Note that $GABA_A$ receptor α1-subunit staining pattern and intensity in the TLE specimen without HS are comparable to those in the autopsy control, yet markedly different from both TLE specimens with HS. *DG*, Dentate gyrus; *H*, dentate hilus; *S*, subiculum. Scale bar, 1 mm.

epilepsy, defined as the interval between onset of habitual seizures and surgical treatment: 28 ± 2.7 years, range, 12–44 years vs 10.4 ± 4.4 years, range, 2–26 years; age at seizure onset: 8.9 ± 1.6 years, range, 1–22 years vs 17.8 ± 4.8 years, range, 9–30 years). A history of an initial precipitating injury (Mathern et al., 1995a), was documented in 11 patients in the HS group and none in the non-HS group. These events included febrile convulsions ($n = 6$), infantile meningitis/encephalitis ($n = 3$), and neonatal anoxia/ischemia ($n = 2$). Preoperatively HS and non-HS patients were on similar antiepileptic medication. Seizure control was assessed in all surgical cases (mean follow-up period of 24 ± 1.1 months). Postoperatively, 12 patients in the HS group (75%) were seizure-free (class 1, as classified after Engel, 1987), two had rare seizures (class 2), and two patients had worthwhile improvement (class 3). In the non-HS group, four patients were seizure-free, and one patient was unchanged. The high success rate in achieving seizure control indicates that the epileptogenic focus was successfully removed with selective amygdalohippocampectomy.

Comparison of patient categories

The distribution of the $GABA_A$ receptor subunits α1, α2, α3, β2,3, and γ2 was analyzed in hippocampal specimens from TLE patients with HS ($n = 16$). For comparison, two control groups were used and defined as hippocampal tissue obtained at autopsy from patients with no evidence of neurological disease ($n = 5$) and tissue surgically removed from patients with TLE, but without HS ($n = 5$). Both were indistinguishable on the basis of morphological criteria except for at most mild neuronal loss in TLE without HS, as reported in previous studies (Babb et al., 1984; Kim et al., 1990). More importantly, the staining pattern for the $GABA_A$ receptor subunits under study was largely similar in the two groups. This is illustrated for the α1-subunit in Figure 1 where the postmortem specimen from a 40-yr-old man with no known neurological disorder (*top left panel*) was compared with the surgical specimen from a 45-yr-old-man with TLE secondary to a benign extrahippocampal tumor and without HS (*bottom left panel*). The origin of control specimens, whether from autopsy or surgery, is indicated in parentheses for each subsequent figure.

To test whether autopsy specimens represent valid controls for surgical specimens, hippocampal tissue obtained at autopsy from a patient with TLE and HS was compared with tissue obtained at surgery from patients suffering from TLE with HS, as shown for $GABA_A$ receptor α1-subunit staining (Fig. 1). Although the autopsy specimen was processed after a 15 hr postmortem interval (*top right panel*) and the surgical specimen immediately after re-

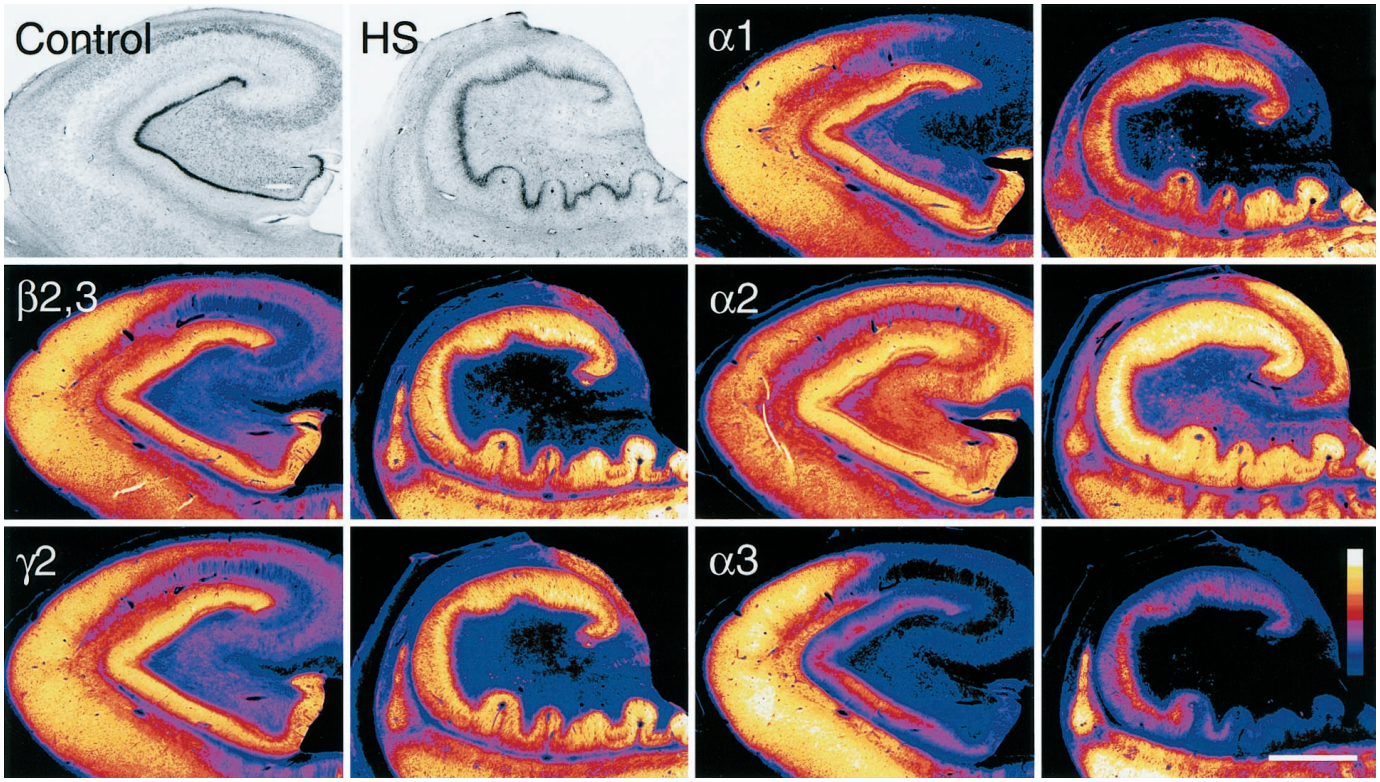

Figure 2. Cytoarchitecture and regional distribution of the major $GABA_A$ receptor subunits in the hippocampus from a control (autopsy, *first* and *third columns*) and a TLE patient with HS (*second* and *fourth columns*). Optical density of staining is color-coded according to a normalized scale showing the strongest signal in *white* and the background in *dark blue*. In both specimens, adjacent sections were stained for the subunits α1, α2, α3, β2,3, and γ2, and for Nissl. In the control, Nissl staining shows a normal distribution of neuronal cell somata. Labeling for the β2,3- and γ2-subunits is largely similar, whereas each α-subunit has a differential distribution pattern. In TLE with HS, Nissl staining reveals prominent cell loss in CA1, CA3, and dentate hilus with relative sparing of the dentate granule cell layer and granule cell dispersion. The CA2 and partly CA3 pyramidal cell layer is not shown in this section, but is visible in those stained for the α-subunits. The decrease in $GABA_A$ receptor subunit immunoreactivity parallels cell loss in CA1, CA3, and dentate hilus, whereas staining is increased or decreased in a subunit-specific manner in CA2 and dentate gyrus. The *magenta* spots in the dentate hilus represent surviving mossy cells. Scale bar, 2 mm.

section (*bottom right panel*), staining patterns were comparable, confirming that $GABA_A$ receptor subunit antigens are stable for several hours after death (Loup et al., 1998).

Regional distribution of $GABA_A$ receptor subunits in controls and TLE with HS

To provide an overview, $GABA_A$ receptor subunits α1, α2, α3, β2,3, and γ2 in the human hippocampus were visualized at low-power magnification in color-coded video images (Fig. 2). Differences in staining intensity for each subunit were assessed using a normalized scale. In rodent brain, these subunits account for at least 80% of all $GABA_A$ receptors (for review, see McKernan and Whiting, 1996; Möhler et al., 1996). Whereas the β2,3- and γ2-subunits are part of most $GABA_A$ receptor subtypes, the α-subunit variants represent largely distinct subtypes with a specific pharmacological profile and distribution pattern. A similar organization in subunit architecture was observed in normal human hippocampus. In control specimens (Fig. 2, *first column*), the β2,3- and γ2-subunits exhibited a comparable labeling pattern, with staining intensity being highest in the dentate molecular layer and CA1, and moderate in CA2, CA3, and hilus. Autoradiographic studies with benzodiazepine radioligands have described a similar distribution of $GABA_A$ receptors, confirming the ubiquitous nature of these two subunits (Faull and Villiger, 1988; Houser et al., 1988; Hand et al., 1997). In contrast, the α-subunit variants showed distinct patterns of immunoreactivity (Fig. 2, *third column*). For the α1-subunit, the density of immunolabeling was highest in the dentate molecular layer and CA1. Staining was moderate in CA2 and hilus. At this level of magnification, CA3 appeared nearly devoid of α1-subunit immunoreactivity. These findings are in accordance with a previous study in normal human tissue (Houser et al., 1988). Immunoreactivity for the α2-subunit was most abundant in the dentate molecular layer. Labeling was also prominent in CA2, CA3, and hilus, and moderate in CA1, a pattern similar to that reported in rodents (Fritschy and Möhler, 1995). Finally, specific α3-subunit immunoreactivity was consistently found to be highest in CA1, moderate to low in CA2, and virtually absent in CA3 and hilus, whereas in the dentate gyrus immunolabeling varied among specimens (see Fig. 13*E,F*). Figure 2 illustrates a case with low α3-subunit immunoreactivity in the dentate molecular layer.

In TLE with HS specimens (Fig. 2, *second* and *fourth columns*), the characteristic pattern of gliosis and regional neuronal loss was revealed with Nissl staining. Cell death was most extensive in CA1 and more moderate in CA3 and dentate hilus, with areas of relative sparing in CA2 and dentate gyrus. Two main alterations in $GABA_A$ receptor subunit expression were observed at the regional level. First, areas of prominent cell loss, such as CA1, CA3, and dentate hilus showed marked reduction in immunoreactivity for all subunits. These changes closely paralleled the pattern of neuronal loss occurring in HS. Second, areas of relative cell loss, such as CA2 and the dentate gyrus, exhibited subunit-specific, increased or decreased intensity of staining in comparison to controls, suggesting corresponding changes in the number of receptors in surviving principal cells. Upregulation was most prominent for the α2-subunit. Differences in staining intensity between HS specimens and the two control groups were assessed by quantitative densitometry in the CA2 pyramidal cell layer and dentate layers (Fig. 3, see below). In the following, results will be described in subregions of the hippocampus in controls and TLE specimens with HS. Unless

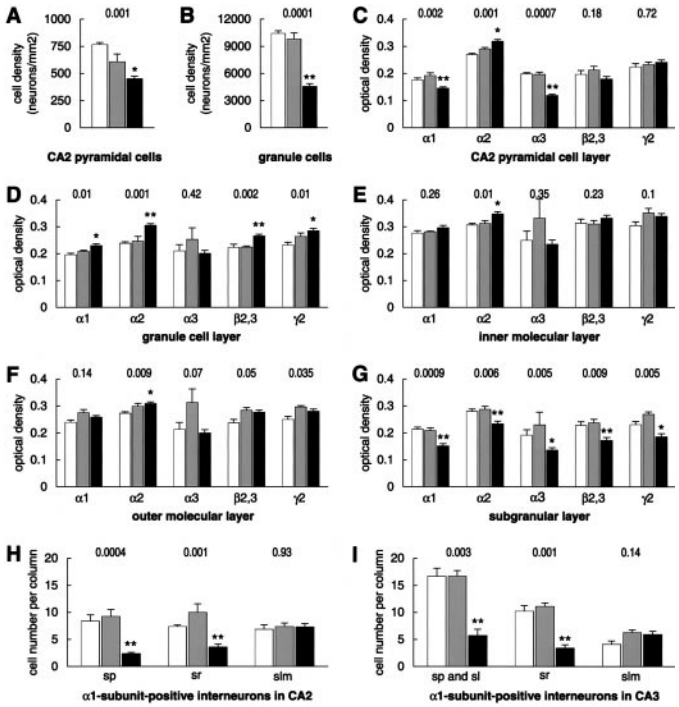

Figure 3. Mean neuronal cell counts and densitometric measurements ± SEM in autopsy (*white bars*), non-HS (*shaded bars*), and HS (*black bars*) patient groups. *A–G,* Sets of six immediately adjacent sections were stained for Nissl and the subunits α1, α2, α3, β2,3, and γ2. *A, B,* Densities of CA2 pyramidal cells (*A*) and granule cells (*B*). *C–G,* Optical density measurements in CA2 pyramidal cell layer (*C*), granule cell layer (*D*), inner molecular layer (*E*), outer molecular layer (*F*), and subgranular layer (*G*). *H, I,* Numbers of α1-subunit-positive interneurons per 625-μm-wide column through each stratum in CA2 (*H*) and CA3 (*I*). Nonparametric ANOVA *p* values are presented above data set, and significant *post hoc* results are indicated by *asterisks* ($p < 0.05$). *Difference compared to the autopsy or non-HS groups; **difference compared to the autopsy and non-HS groups.

otherwise mentioned, the distribution of the ubiquitously present β2,3- and γ2-subunits largely paralleled that found for the α-subunit variants and will not be described further.

$GABA_A$ receptor subtypes in the CA1 area

Control specimens

Within CA1, a laminar pattern was observed for all subunits, as illustrated in Figure 4*A* for the α2-subunit and Figure 4*D* for the α1-subunit. Stratum pyramidale showed highest intensity and strata oriens and lacunosum-moleculare moderate intensity of staining. Because of the fused hippocampal fissure, labeling of stratum lacunosum-moleculare often appeared continuous with that of the dentate molecular layer (Fig. 4*A*). The more lightly stained band represented stratum radiatum. Immunoreactivity was diffusely present throughout the pyramidal cell and dendritic layers. At high magnification, individual pyramidal neurons could be discerned, outlined by discrete staining along the surface of the somata and proximal dendrites (data not shown; Loup et al., 1998). Among all subunits, α3-subunit immunoreactivity was highest, a finding that contrasts with data from rodents, in which α3-subunit staining is absent in CA1 (Fritschy and Möhler, 1995; Sperk et al., 1997).

An important additional feature of α1-, and less prominently β2,3- and γ2-subunit immunoreactivity in the hippocampus was the intense labeling of numerous nonpyramidal cells. Based on their size, location, and dendritic arborization, several types of interneurons could be distinguished. Because of the strong neuropil staining in CA1, it was not always possible, however, to identify them all. In stratum oriens, somata of many immunoreactive neurons were fusiform with long dendrites that ran parallel to the alveus, or round with few, short dendrites. These cells were superimposed on a dense network of immunoreactive dendrites. In stratum pyramidale, large and intensely stained multipolar cells were seen with their dendrites passing through the strata pyramidale and radiatum before entering the stratum lacunosum-moleculare (Fig. 5*A*). Most conspicuous was the presence of small round interneurons, which were especially numerous in stratum lacunosum-moleculare (Fig. 4*D*). Their radially oriented dendrites, forming a fine network superimposed on diffuse neuropil, conferred a stellate-like aspect to these cells.

TLE specimens with HS

In this series, three of 16 specimens showed segmental conservation of the CA1 pyramidal cell layer (Figs. 2, 4*B*), in which atrophy was partial, and the staining pattern in the preserved area was similar to that of control specimens. In the other 13 specimens, there was marked atrophy of the CA1 area (Fig. 4*C*, α2-subunit, *E*, α1-subunit). Whereas strata pyramidale and radiatum were reduced to a thin band virtually devoid of pyramidal cells, stratum lacunosum-moleculare largely retained its original size. The few surviving pyramidal cells were faintly immunoreactive for $GABA_A$ receptors (data not shown).

In the absence of immunoreactivity in the dendritic fields of the degenerated pyramidal cells, the interneurons expressing the α1-subunit were revealed in all specimens (Figs. 4*E*, 5*B*,*C*). In stratum oriens, fusiform, round, and multipolar interneurons could be observed within a dense network of dendrites (Fig. 4*E*). In strata pyramidale and radiatum, several types of nonpyramidal cells could be distinguished with somata that were small and round, medium-sized, or large and multipolar. The latter cell type frequently displayed irregular soma conformations and dendrites that appeared tangled, nodulated, variable in their diameters, and increased in number (Fig. 5*B*,*C*). Finally, stratum lacunosum-moleculare contained numerous small interneurons whose dendrites formed a more intricate network than that observed in controls. Occasional round cells of moderate size were also seen (Fig. 4*E*).

Because of prominent neuropil labeling in control tissue, which largely prevented counts of α1-subunit-positive interneurons in the different strata, it was not possible to evaluate the extent, if any, of interneuron loss that had occurred in HS specimens. As illustrated in Figure 4*E*, however, interneurons present in strata pyramidale and radiatum were consistently less numerous than in stratum lacunosum-moleculare in the CA1 area.

$GABA_A$ receptor subtypes in the CA2 area

Control specimens

A subunit-specific pattern of staining was observed in the CA2 area. The α2-subunit exhibited a laminar distribution comparable to that in CA1, with intense staining in stratum pyramidale and lightest staining in stratum radiatum (Figs. 2, 6*C*). α3-Subunit immunoreactivity was very different, in that it mainly outlined the cell bodies of a few pyramidal neurons in the superficial aspect of the stratum pyramidale. In stratum radiatum, their lightly labeled apical dendrites formed delicate processes that ran parallel to one another and entered the stratum lacunosum-moleculare where staining was more diffuse (Fig. 6*E*). A laminar pattern was also seen for the α1-subunit (Figs. 1, 2, 7*A*).

In addition, as in CA1, α1-subunit immunoreactivity revealed a population of interneurons that were readily visible because of the low to moderate α1-subunit-positive neuropil in CA2. In stratum oriens, strong immunolabeling of fusiform and large multipolar somata was detected. Their dendrites mostly ran parallel to the alveus and frequently formed a dense fiber network. In stratum pyramidale, three types of nonpyramidal neurons were identified (Fig. 7*A*,*D*): (1) large, intensely stained multipolar interneurons with long apical and basal dendrites, (2) medium-sized, oviform cells with apical dendrites that could be followed into stratum radiatum, and (3) small round interneurons. In stratum radiatum, a few round and medium-sized α1-subunit-positive interneurons were seen. In addition, strongly stained individual, or fascicles of, dendritic processes passed through stratum radiatum and entered

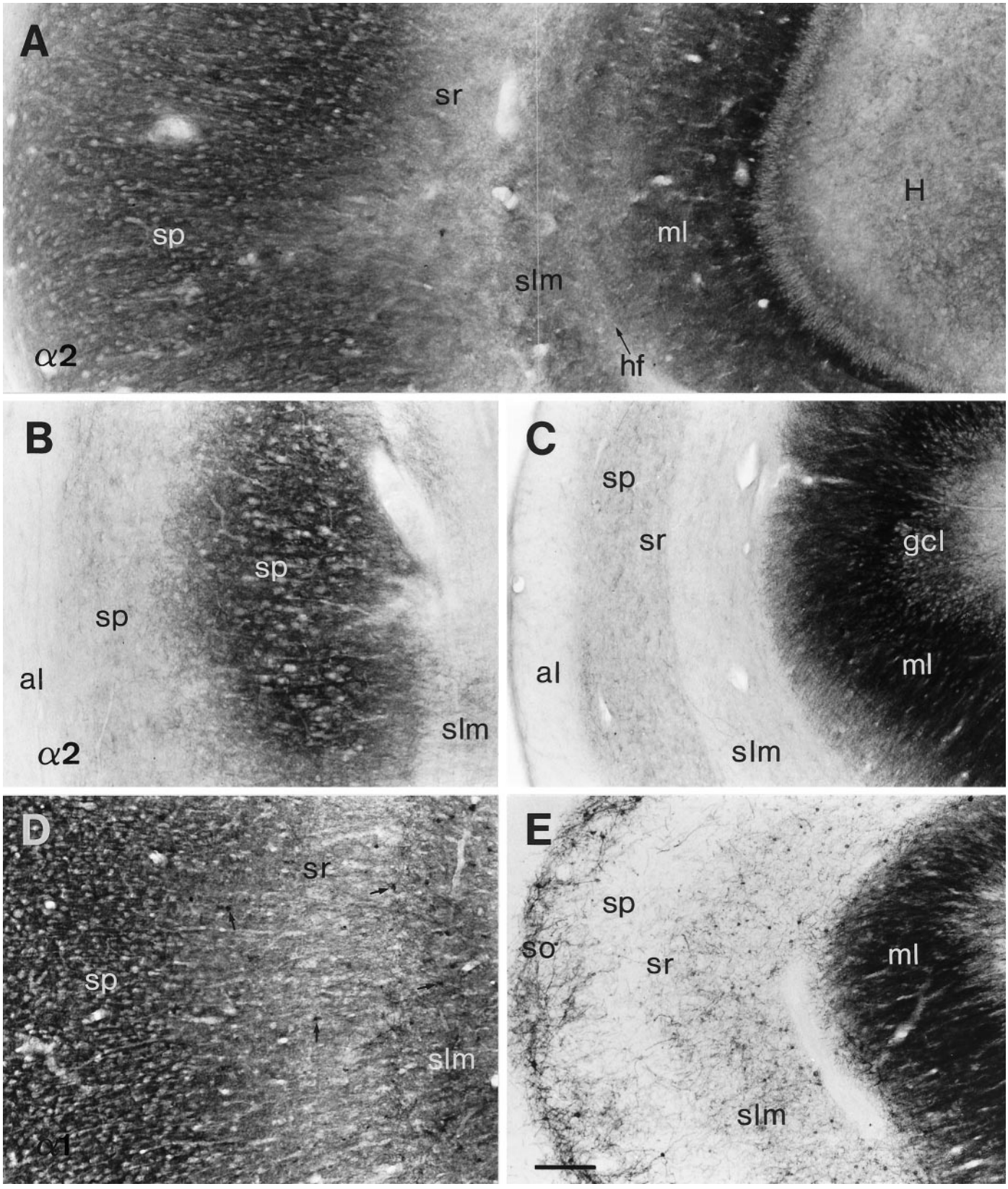

Figure 4. Subunit-specific $GABA_A$ receptor immunoreactivity in the CA1 area of controls (*A, D*, autopsy) as compared to TLE with HS (*B, C, E*). *A, D,* Control sections exhibit a laminar staining pattern for the α2- and α1-subunits, respectively. Whereas immunoreactivity for both subunits is diffusely distributed in neuropil, α1-subunit immunoreactivity is also present in numerous nonpyramidal neurons (*D, arrows*). *B, C,* Sections from two HS specimens stained for the α2-subunit, where in *B* the partly conserved CA1 pyramidal cell layer shows α2-subunit immunoreactivity, and in *C* there is almost complete pyramidal cell loss associated with severe atrophy of the CA1 area. *E,* Section from an HS specimen stained for the α1-subunit, showing the loss of neuropil staining and the layer-specific distribution of nonpyramidal neurons. Whereas small interneurons are conserved in stratum lacunosum-moleculare and larger interneurons in stratum oriens, few interneurons are visible in strata pyramidale and radiatum. Note the increase in $GABA_A$ receptor α2- and α1-subunit expression in dentate molecular and granule cell layers in HS specimens. *al*, Alveus; *gcl*, dentate granule cell layer; *H*, dentate hilus; *hf*, hippocampal fissure; *ml*, dentate molecular layer; *slm*, stratum lacunosum-moleculare; *so*, stratum oriens; *sp*, stratum pyramidale; *sr*, stratum radiatum. Scale bar, 200 μm.

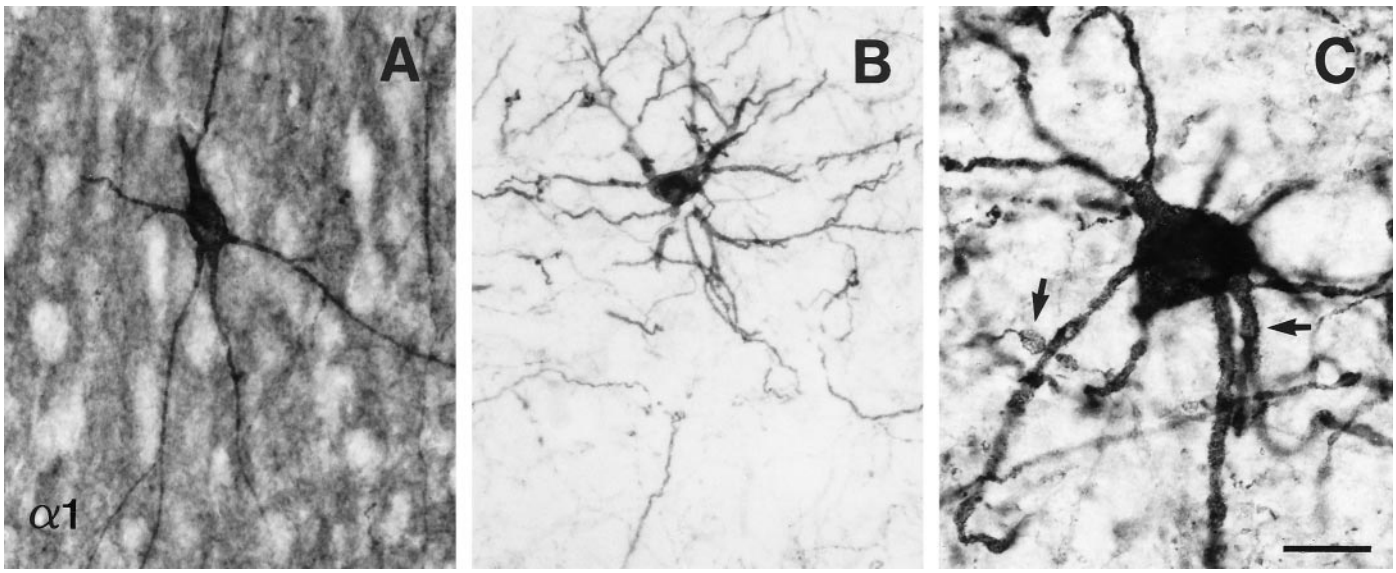

Figure 5. Altered morphology of large multipolar interneurons immunoreactive for the α1-subunit in the CA1 pyramidal cell layer in TLE with HS. *A*, In the autopsy control, soma contours are smooth with few long and straight dendrites. *B, C,* In HS specimens, the soma exhibits an irregular shape, and dendrites appear tangled, variable in their diameters, and increased in number. At higher magnification (*C*), dendritic nodulations are visible (*arrows*). Note the absence of α1-subunit staining in neuropil reflecting severe pyramidal cell loss in CA1. Scale bar: *A, B,* 50 μm; *C,* 25 μm.

stratum lacunosum-moleculare (Fig. 7*A*). Stratum lacunosum-moleculare contained a number of small stellate-shaped interneurons with four to eight dendrites forming a delicate network against a lightly stained diffuse neuropil (Fig. 7*A,G*). At the border between stratum lacunosum-moleculare and the dentate molecular layer, occasional medium-sized cells were observed with smooth dendrites oriented in a horizontal plane (data not shown).

TLE specimens with HS

Considerable reorganization in $GABA_A$ receptor subtype distribution was observed in the CA2 area. Despite an average 40% loss in pyramidal cells (Figs. 3*A*, 6*B*), stronger α2-subunit immunoreactivity than in control tissue was present in the surviving pyramidal cells and dendritic fields (Fig. 6*D*). At high-power magnification, intense staining was seen to outline their somata, which were frequently deformed in shape and arranged in a disorganized manner. Furthermore, a striking rearrangement of α3-subunit immunoreactivity occurred. Intense immunolabeling adorned individual thickened apical dendrites passing through stratum radiatum, whereas pyramidal cell bodies were virtually unstained (Fig. 6*F*). Tangentially cut processes could be observed in strata radiatum and lacunosum-moleculare, indicating a change in direction of some apical dendrites along the rostrocaudal axis.

Alterations in α1-subunit immunoreactivity markedly differed in pyramidal versus nonpyramidal cells. Pyramidal cells and dendritic layers displayed decreased and more diffuse staining in comparison to control tissue (Figs. 1, 7*B,C*). In contrast, extensive layer-specific changes in α1-subunit-positive interneurons were seen for all HS specimens. In strata pyramidale and radiatum, profound loss of the small, round and medium-sized interneurons immunopositive for the α1-subunit was observed (Fig. 7*B,C,E*), whereas the large multipolar nonpyramidal cells remained for the most part. However, their somata were deformed, and the dendritic arborization was altered (Fig. 7*E,F*). In contrast, in stratum lacunosum-moleculare the numerous small, round interneurons were preserved and surrounded by a dense dendritic network (Fig. 7*B,C,H,I*). Furthermore, the fusiform somata of interneurons present at the border between stratum lacunosum-moleculare and the dentate outer molecular layer frequently appeared larger and more irregular than in control tissue, and their dendrites were more prominent.

Quantitative analysis

In addition to neuron counts performed in adjacent Nissl-stained sections (Fig. 3*A*), differences in staining intensity between the autopsy, non-HS, and HS groups were assessed quantitatively by densitometry for each of the five subunits in the CA2 pyramidal cell layer (Fig. 3*C*). The following observations were made: (1) HS specimens showed decreased neuron densities when compared to autopsy ($p < 0.01$), and a similar trend was observed when compared with non-HS cases, whereas the difference between the autopsy and non-HS groups was not significant. (2) There were subunit-specific differences in OD for the α-subunit variants α1, α2, and α3. Compared with the autopsy group, α2-subunit OD in HS was significantly increased ($p < 0.01$), whereas OD for the α1- and α3-subunits was significantly decreased ($p < 0.05, p < 0.01$, respectively). Furthermore, OD for the α1- and α3-subunits was significantly decreased compared to the non-HS group ($p < 0.01, p < 0.05$, respectively). (3) No significant difference in OD was found for all three α-subunit variants between the autopsy and non-HS groups. (4) As for the ubiquitously present β2,3- and γ2-subunits, no significant difference in OD was found between the three patient categories, which may reflect a change in receptors containing these subunits, whereby a decrease in one subtype of receptor (α1 or α3) is compensated for by an increase in another (α2). These findings suggest that while the total number of receptors may not change significantly in the CA2 area in HS specimens, the relative proportion of α2-subunit-containing $GABA_A$ receptors is markedly increased.

To verify the observed loss or preservation of α1-subunit-positive interneurons in specific strata, counts were performed in 625-μm-wide columns through each stratum in the three patient categories (Fig. 3*H*). In strata pyramidale and radiatum, the HS group showed decreased numbers of α1-subunit-positive interneurons when compared with the autopsy or non-HS specimens (stratum pyramidale: $p < 0.01, p < 0.05$, respectively; stratum radiatum: $p < 0.05$ for both). In contrast, in stratum lacunosum-moleculare, the number of α1-subunit-positive interneurons was not significantly different in the HS group when compared with the autopsy and non-HS specimens. For all strata, no significant difference in interneuron counts was found between the autopsy group and non-HS cases. These statistical data confirm the observation that,

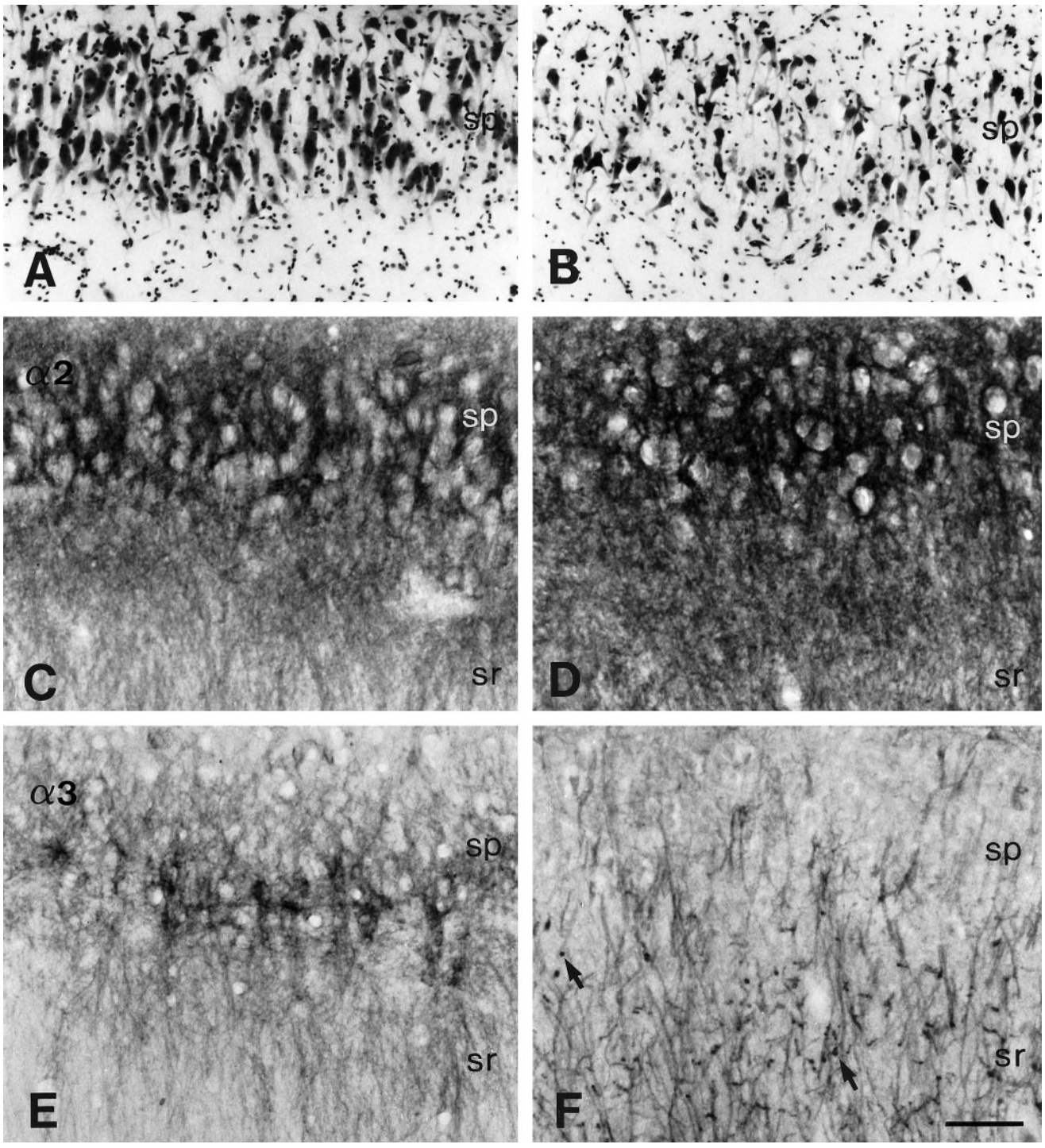

Figure 6. Subunit-specific alterations in $GABA_A$ receptor immunoreactivity in the CA2 area in controls (*A, C*, autopsy; *E*, surgery, TLE without HS) versus TLE with HS (*B, D, F*). *A, B,* Nissl-stained sections show moderate pyramidal cell loss in TLE with HS (*B*) as compared to control hippocampus (*A*). *C, D,* α2-subunit immunoreactivity is increased in surviving pyramidal cells in TLE with HS (*D*) in comparison to controls (*C*). *E, F,* Redistribution of α3-subunit immunoreactivity. In control hippocampus (*E*), staining is prominent, outlining the somata of a few pyramidal cells, but weak in their apical dendrites, whereas in TLE with HS (*F*), thickened apical dendrites show intense immunoreactivity with virtually absent labeling of somata. Note the tangentially cut dendrites reflecting disorganization in orientation (*arrows*). Abbreviations, see Figure 4. Scale bar, 100 μm.

in the HS group, a significant number of α1-subunit-positive interneurons are lost in strata pyramidale and radiatum while they are preserved in stratum lacunosum-moleculare.

$GABA_A$ receptor subtypes in the CA3 area

Control specimens

In the CA3 area, abundant α2-subunit immunoreactivity was distributed in a laminar pattern largely similar to that in CA1 and CA2 (Fig. 8*A*). Neuropil staining was, however, more prominent and less diffuse, except in strata radiatum and lucidum where it was fainter. Immunolabeling for the α3-subunit was virtually absent (Fig. 2). Likewise, faint or no α1-subunit staining was observed on the pyramidal cell bodies and dendritic fields (Figs. 2, 9*A*). In contrast, numerous interneurons expressing this subunit were detected in CA3 (Figs. 8*C,E,* 9*A*). The types of nonpyramidal neurons labeled and the distribution pattern in CA3 were largely similar to those in CA2. Their darkly stained dendrites were of variable calibers, usually running toward stratum lacunosum-moleculare and stratum

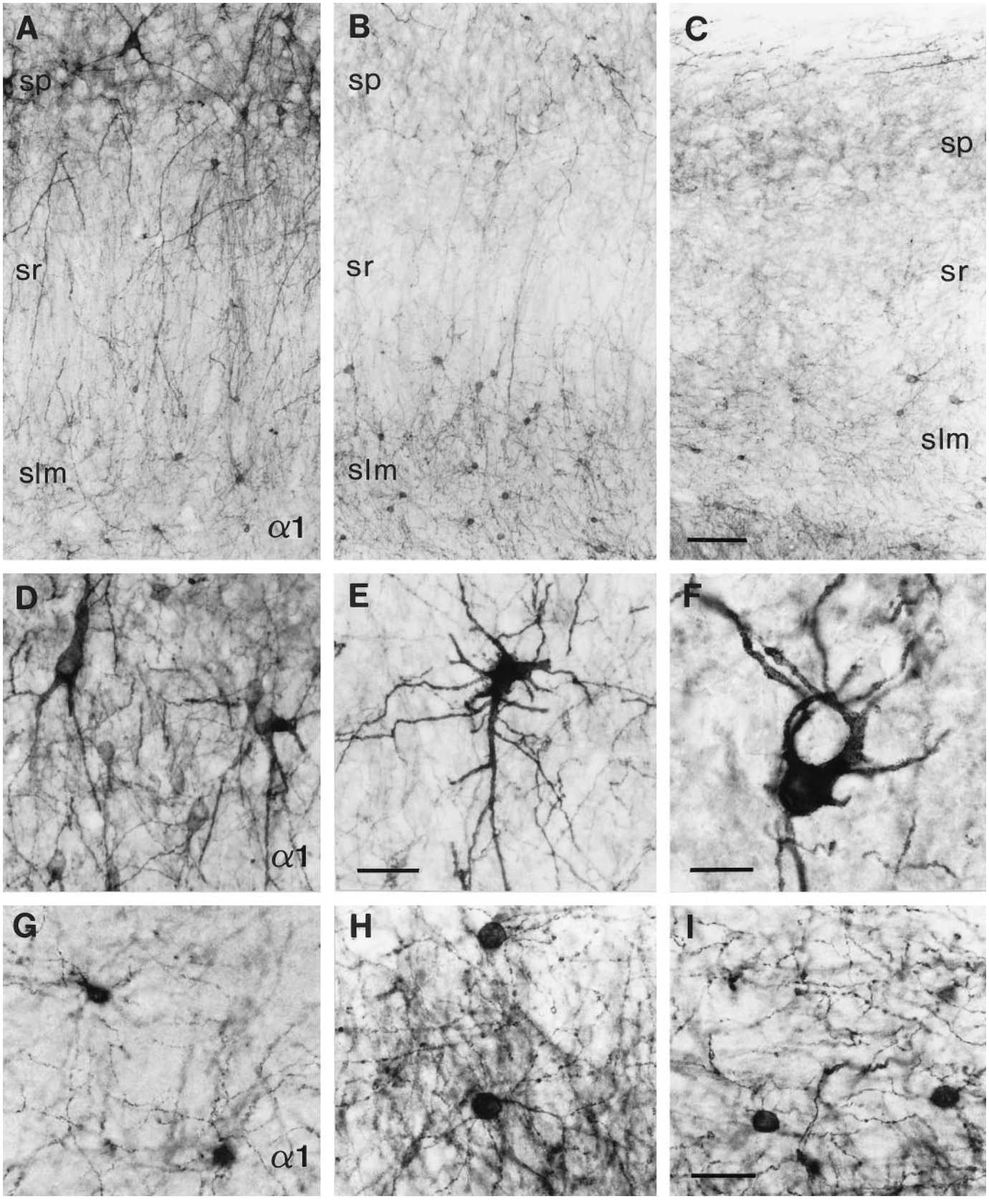

Figure 7. Layer-specific changes in interneurons stained for the $GABA_A$ receptor α1-subunit in the CA2 area in five different TLE specimens with HS (*B, C, E, F, H, I*) versus three different controls (*A, G*, autopsy; *D*, surgery, TLE without HS). *A–C,* Overview; *D–F,* stratum pyramidale; *G–I,* stratum lacunosum-moleculare. *A, D, G,* In controls, several types of nonpyramidal cells are found in strata pyramidale and radiatum, whereas predominantly small interneurons are present in stratum lacunosum-moleculare. *B, C,* In TLE with HS, the loss of interneurons in strata pyramidale and radiatum is either extensive (*B*) or virtually complete (*C*), whereas the small interneurons are conserved in stratum lacunosum-moleculare. *E, F,* In stratum pyramidale, surviving interneurons are large and display prominent somatic and dendritic alterations, whereas other types of interneurons are no longer apparent. *H, I,* In stratum lacunosum-moleculare, the small interneurons are preserved, exhibiting an intricate dendritic network. Abbreviations, see Figure 4. Scale bars: *A–C,*100 μm; *D, E,* 50 μm; *F–I,* 25 μm.

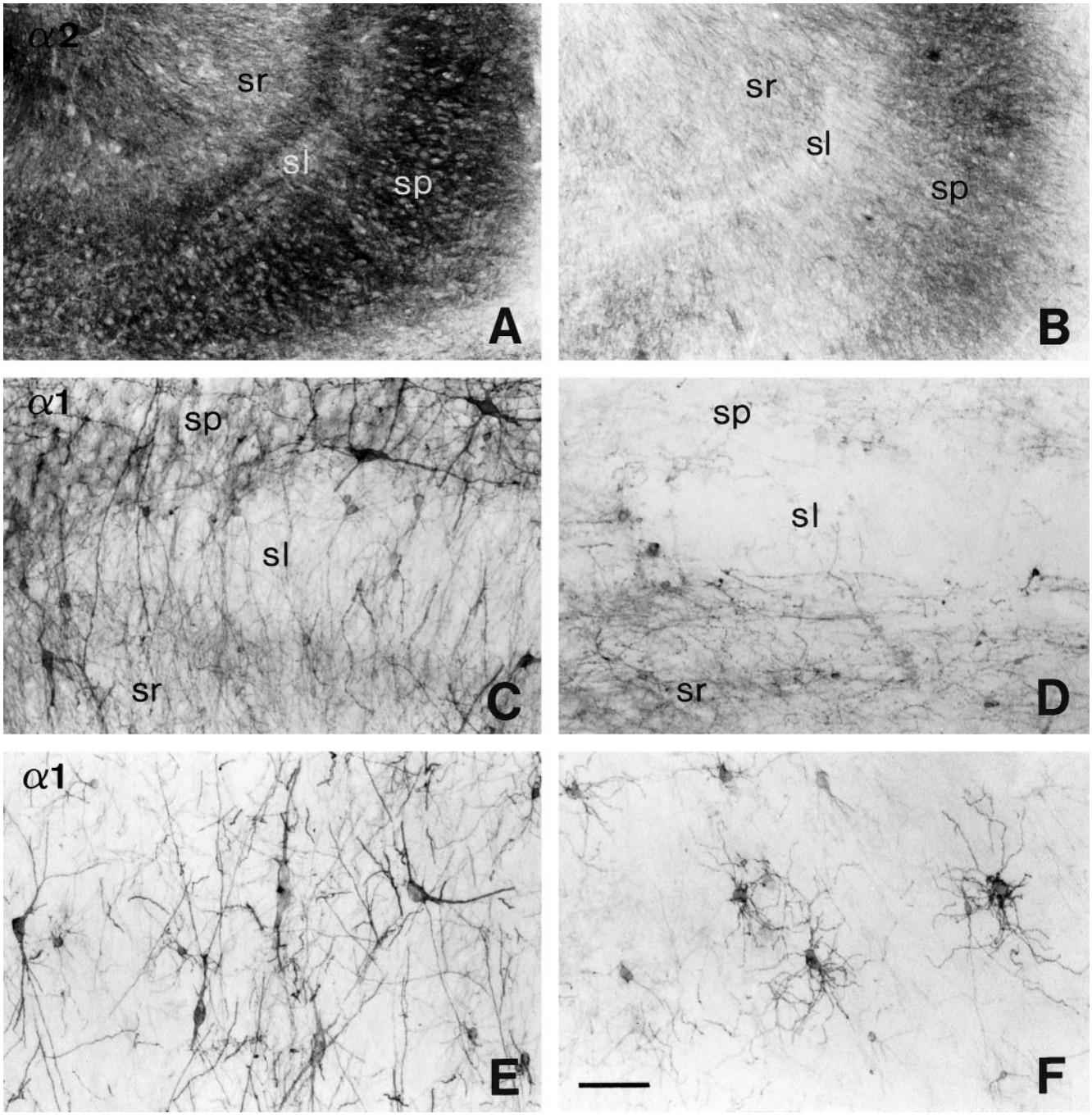

Figure 8. Subunit-specific changes in $GABA_A$ receptor immunoreactivity in the CA3 area in controls (*A, E*, autopsy; *C*, surgery, TLE without HS) as compared to TLE with HS (*B, D, F*). *A, B,* α2-subunit, overview. *C–F,* α1-subunit with part of CA3 bordering CA2 (*C, D*) and part of CA3 inserting into the dentate hilus (*E, F*). *A,* A control section showing the laminar staining pattern with prominent labeling in stratum pyramidale and lighter labeling in strata lucidum (*sl*) and radiatum. *B,* Section from a HS specimen with segmental, moderate to light staining reflecting the moderate to severe pyramidal cell loss. *C,* In the control, whereas different types of α1-subunit-positive interneurons are present in strata pyramidale and radiatum, small oviform neurons are found in stratum lucidum. *D,* In TLE with HS, there is marked loss of interneurons in these strata. *E,* In stratum pyramidale of the control, large multipolar interneurons with dendrites oriented perpendicularly to the pyramidal cell layer stand out against a fine dendritic network. *F,* In TLE with HS, the few surviving interneurons located in stratum pyramidale have undergone extensive morphological transformation. Their fine dendrites appear tangled, increased in number, and radially oriented. Abbreviations, see Figure 4. Scale bar: *A, B,* 200 μm; *C–F,* 100 μm.

oriens, but also without preferred direction. In addition, interneurons with round to oval cell bodies and fine dendrites were observed in stratum lucidum (Fig. 8*C*). Conspicuously, interneurons were most numerous at the border between strata pyramidale and lucidum.

TLE specimens with HS

In contrast to the increased $GABA_A$ receptor α2-subunit immunoreactivity described for the CA2 area, staining intensity for this subunit paralleled the degree of pyramidal cell loss in CA3, suggesting that no upregulation occurs in CA3 pyramidal cells (Fig. 8*B*). Considerable cellular disorganization was apparent in stratum pyramidale, where somata were poorly aligned to each other and exhibited various shapes. In three cases, pyramidal neurons were largely preserved, and staining was similar to control tissue (data not shown). In the other specimens, pyramidal cell loss was moderate to severe and frequently segmental, mostly in the part of CA3 inserting into the dentate hilus (Fig. 8*B*).

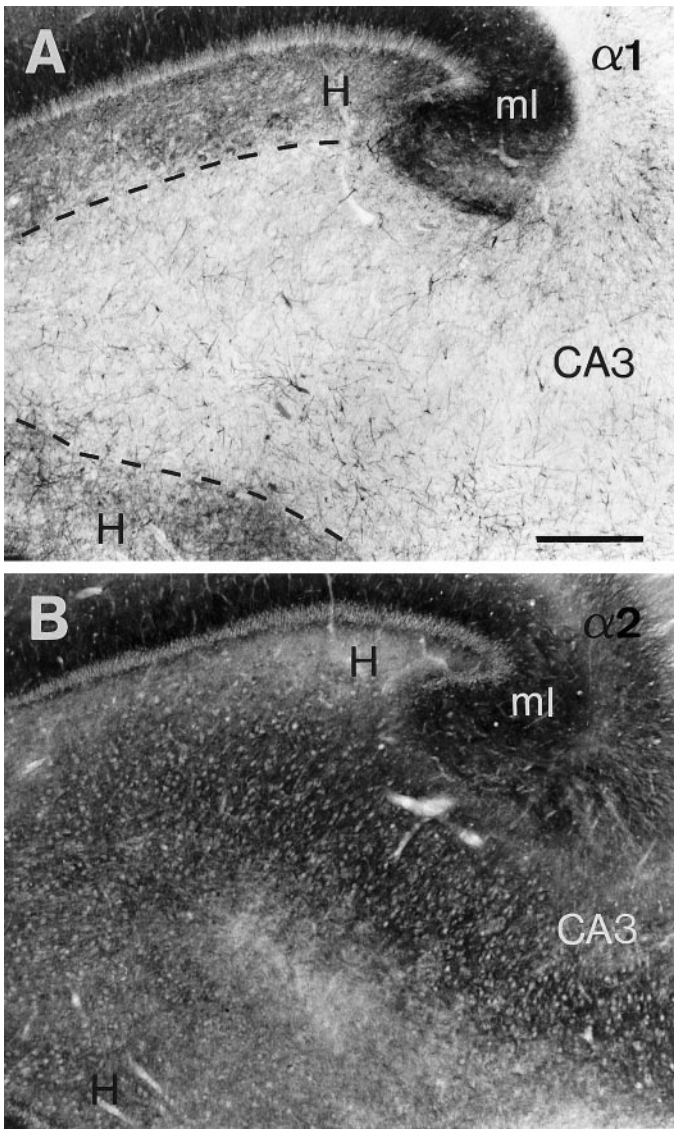

Figure 9. Differential distribution of α1- and α2-subunit immunoreactivity in dentate hilus and CA3 in hippocampal tissue obtained at autopsy. *A,* Moderate α1-subunit staining is present in the hilus, whereas the CA3 area appears faintly labeled. The abrupt change in staining intensity allows the boundary between the hilus and the CA3 area to be readily distinguished (*dashed line*). *B,* In contrast, moderate α2-subunit staining is equally present in both regions where the lighter spots represent neuronal cell bodies. Even at this low-power magnification, a trilaminate pattern can be discerned within the hilus. *A* and *B* are adjacent sections. Scale bar, 0.5 mm.

Layer-specific changes were observed for α1-subunit-positive interneurons, which were comparable to those in CA2. Marked loss of these interneurons was observed in strata pyramidale, lucidum, and radiatum, and especially at the border between strata pyramidale and lucidum (Fig. 8*D*). When large multipolar interneurons were preserved in stratum pyramidale, their somata were frequently encrusted with intense α1-subunit staining (Fig. 8*F*). Instead of exhibiting a few long dendrites oriented perpendicularly to the pyramidal cell layer as in controls (Fig. 8*E*), these interneurons displayed more numerous, shorter dendrites that ran in a radial direction. In contrast, small, round interneurons morphologically identical to those found in CA1 and CA2 were also preserved in CA3 stratum lacunosum-moleculare.

Quantitave analysis

As in CA2, the numbers of α1-subunit-positive interneurons were quantitatively assessed in distinct strata in the three patient groups (Fig. 3*I*). Strata pyramidale and lucidum, however, were considered together, because most interneurons were present at the border between both strata and, therefore, could not be attributed unambiguously to one or the other stratum. In strata pyramidale-lucidum and radiatum, the HS group showed decreased numbers of α1-subunit-positive interneurons when compared with the autopsy or non-HS specimens (stratum pyramidale-lucidum: $p < 0.01$, $p < 0.05$, respectively; stratum radiatum: $p < 0.01$, $p < 0.05$, respectively). In contrast, in stratum lacunosum-moleculare, the number of α1-subunit-positive interneurons was not significantly different in the HS group as compared to the autopsy or non-HS specimens. For all strata, no significant difference in interneuron counts was found between the autopsy group and non-HS cases. Thus, statistically significant layer-specific changes in the number of α1-subunit-positive interneurons in HS were present in CA3 as well.

$GABA_A$ receptor subtypes in the dentate hilus

Control specimens

In the dentate hilus, the $GABA_A$ receptor distribution pattern was found to be subunit-specific, as in the hippocampal fields (Fig. 2). The boundary between the hilus and CA3, which often is quite difficult to delineate, was readily recognized as an abrupt transition of α1-subunit staining. Thus, α1-subunit immunoreactivity was moderate in dentate hilus but weak in CA3 (Figs. 2, 9*A*). In contrast, α2-subunit immunoreactivity was of relatively similar intensity in these two regions (Fig. 9*B*). Within the dentate hilus, a trilaminate pattern was observed for both the α2- and α1-subunits, as well as the ubiquitously present β2,3- and γ2-subunits (Figs. 4*A*, 9*A,B,* 10*D,G*). First, a layer of prominent diffuse neuropil staining, the subgranular layer, was observed immediately subjacent to the granule cell layer and represented the basal dendrites of granule cells (see "$GABA_A$ receptor subtypes in the dentate gyrus"). Second, a weakly labeled neuron-sparse zone of variable thickness could be identified. Third, a region that comprised the majority of the hilar cells, the polymorphic layer, was situated deep to this zone. In the case of α2-subunit staining, the hilar neurons frequently appeared as white spots at low-power magnification, surrounded by a moderately immunoreactive neuropil (Fig. 9*B*). In contrast, α1-subunit-positive cell bodies and an associated network of dendrites were intensely stained and surrounded by a moderately to lightly immunoreactive neuropil (Figs. 9*A*, 10*D*).

The dentate hilus contains a variety of neuronal cell types with unique morphological features, as reported in rat (Amaral, 1978) and human brain (Braak, 1974; al-Hussain and al-Ali, 1995; Blümcke et al., 1999). In the present study, a large number of hilar cells immunopositive for either the α1-, α2-, or α3-subunit, or both the α1- and α2-subunits were identified, based on the comparison of adjacent sections stained for these subunits. Unexpectedly, previously undescribed pyramidal-shaped neurons immunoreactive for the α2-subunit were observed well within the hilar borders. At higher magnification, discrete staining occurred along the surface of the somata and proximal dendrites, and intense staining revealed darkly stained longitudinal processes 20- to 40-μm-long (Fig. 10*A*). Using confocal laser-scanning microscopy, these structures were putatively identified as axon initial segments intensely immunoreactive for the α2-subunit (Loup et al., 1998). The most prominent type of hilar cell was the mossy cell, which exhibited strong staining for both the α2- and α1-subunits (Fig. 10*D*; Loup et al., 1998). The mossy cells were readily distinguished by the presence of characteristic "clusters of spheres" that form the mossy cell thorny excrescences, as described by Amaral (1978). Finally, a number of putative interneuron cell types immunopositive for the α1-subunit were seen, including large multipolar cells. These were localized in the polymorphic and subgranular layers (Fig. 10*D*,*G*), and their dendrites traveled for long distances within the hilus or ascended far into the dentate molecular layer. Occasionally large multipolar interneurons with long dendrites were observed that were stained lightly for the α3-subunit. Otherwise, no specific staining was detected in the polymorphic layer for this subunit.

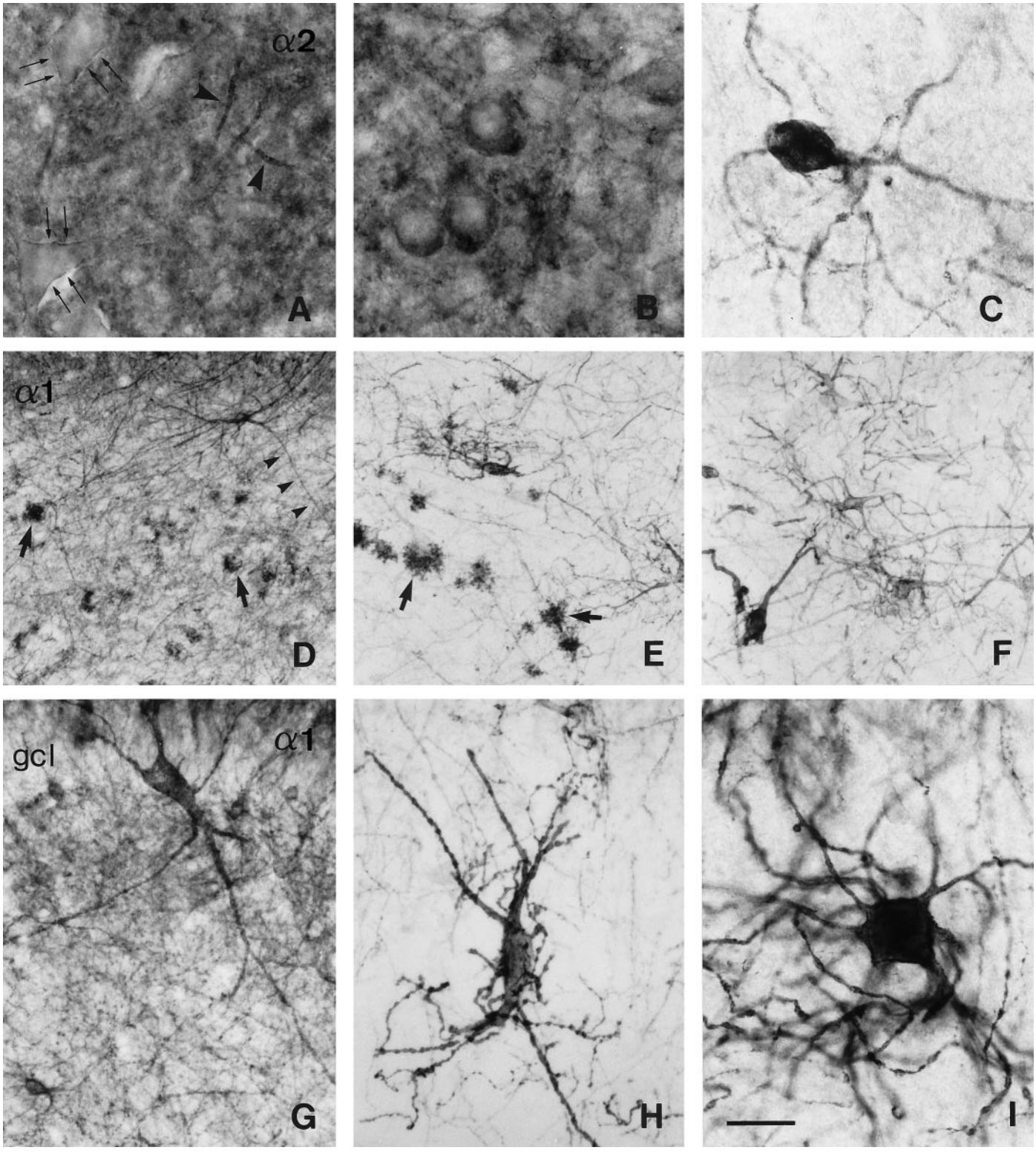

Figure 10. Alterations in $GABA_A$ receptor α2- and α1-subunit immunoreactivity in the dentate hilus in TLE with HS (*B, C, E, F, H, I*) versus controls (*A, D*, autopsy; *G*, surgery, TLE without HS). α2-subunit (*A–C*), α1-subunit (*D–I*). *A,* In the control, α2-subunit labeling discretely outlines the somata of pyramidal-shaped neurons (*double arrows*), whereas intense staining reveals their axon initial segments (*large arrowheads*). *B, C,* HS specimens. In *B*, oval neurons with intense α2-subunit immunoreactivity along the somata resulting in a thickened outline are superimposed on decreased neuropil staining. In *C*, a surviving medium-sized neuron exhibits α2-subunit staining against the white background because of severe loss of neuropil and cells. *D, G,* In controls, light neuropil staining is present with several cell types immunoreactive for the α1-subunit, including mossy cells (*arrows*) and large multipolar interneurons with long dendrites (*small arrowheads*). *E, F,* In TLE with HS, neuropil staining is absent, and cell loss has occurred; among the surviving cells, mossy cells (*E, arrows*) and large interneurons with irregular somata and disorganized tangled dendrites can be recognized. *G–I,* The altered morphology of large multipolar interneurons located in the subgranular layer is shown at higher magnification in two HS specimens (*H, I*) as compared to a control specimen (*G*). In TLE with HS, these interneurons often display changes in soma shape and dendritic arborization including coiling, nodulation, strong variation in calibers, and increased ramification. Scale bar: *A–C, I,* 25 μm; *D–F,* 100 μm; *G, H,* 50 μm.

TLE specimens with HS

In the polymorphic layer, the degree of neuronal loss was variable, with cell loss being mild to moderate in five cases and severe in the other specimens. In cases of lesser cell loss, the neuropil showed decreased α2-subunit immunoreactivity, and round hilar cells could be seen with their somata frequently outlined by intense staining (Fig. 10*B*). These neurons were unstained for the α1-subunit in adjacent sections (data not shown). In cases of marked cell loss, staining intensity of the neuropil for both the α1- and the α2-subunits was reduced to virtually nondetectable levels. Surviving hilar neurons and their dendritic network thus appeared darkly stained against the pale background and were easily recognized (Fig. 10*C,E,F*). Preserved cell types included: (1) α1- and α2-subunit-positive mossy cells (Figs. 2, *fourth column*, 10*E*). Despite severe loss, mossy cells were the most numerous among the surviving α2-subunit-positive hilar neurons and represented a sizable portion of the surviving α1-positive hilar neurons; (2) α2-subunit-positive oviform cells with dendrites extending over long distances (Fig. 10*C*); and (3) α1-subunit-positive large multipolar interneurons, with irregular cell bodies and dendrites that appeared tangled, nodulated, and increased in number (Fig. 10*E,F,H,I*). No specific soma staining was visible for the α3-subunit against the white background.

$GABA_A$ receptor subtypes in the dentate gyrus

Control specimens

Cell type-specific $GABA_A$ receptor subunit distribution was also observed in the dentate granule cells. Staining for the α1-, α2-, β2,3-, and γ2-subunits was prominent in the apical dendritic field forming the molecular layer and appeared stronger in the inner as compared to the outer part (Fig. 2, *first* and *third columns*). The dentate molecular layer displayed a higher intensity of staining than any other area of the hippocampus (Fig. 2, *first* and *third columns*). In the subgranular layer, diffuse moderate labeling was observed in the basal dendritic field (Figs. 4*A*, 9*A,B,* 11*A,C*). In contrast to the marked staining of both apical and basal dendritic trees, labeling barely outlined the somata of the tightly packed granule cells (Figs. 11*A,C,* 12, 13*A,D*). Whereas the α1-, α2-, β2,3, and γ2-subunits showed a largely similar distribution pattern in the dentate gyrus of all specimens, α3-subunit expression was variable. Despite similar intensity of staining in the CA1 area for all cases (as exemplified in Fig. 2, *third column*), in granule cells this subunit showed patchy labeling ranging from very weak (Fig. 11*E*) to high levels of density (Fig. 11*F*) along the somata and basal and apical dendritic fields. These case-specific variations were not dependent on age, postmortem interval, or general quality of tissue, suggesting a propensity for plasticity in α3-subunit immunoreactivity in dentate granule cells.

As in the hippocampal fields and dentate hilus, α1-, and less prominently β2,3- and γ2-subunit staining revealed nonpyramidal cells in the granule cell and molecular layers. In particular, small round interneurons similar to those described in stratum lacunosum-moleculare of the hippocampus proper were observed. Finally, darkly stained processes were frequently seen coursing through the granule cell layer, originating from interneurons mostly located in dentate hilus, but also in the granule cell and molecular layers (Fig. 10*D,G*).

TLE specimens with HS

Marked alterations in the distribution pattern and staining intensity of the α1-, α2-, β2,3-, and γ2-subunits were observed in the granule cell layer and dendritic fields. At low-power magnification, the molecular layer displayed prominent staining, standing out against the relatively weakly labeled hippocampal fields and hilus (Figs. 1, 2). Staining appeared conserved or augmented when compared to control specimens, despite a >50% loss in granule cells (Fig. 3*B*), suggesting the presence of more $GABA_A$ receptors on surviving apical dendrites. Of all subunits, α2 exhibited the largest increase, as illustrated for eight cases (Figs. 2, *fourth column*, 12). For specimens with moderate granule cell loss, the intensity of labeling measured in the molecular layer was higher than that in control specimens. For specimens with severe granule cell loss, the apparent intensity was similar to that in control specimens. α1-, β2,3-, and γ2-subunit immunoreactivity was conserved or increased, but not as markedly (Figs. 1, 2, *second* and *fourth columns*). In contrast, α3-subunit labeling was variable as in the controls, being either faint (Fig. 11*G*) or intense (Fig. 11*H*). For all subunits, changes in staining intensity were most pronounced in the inner portion of the molecular layer along a thin band immediately adjacent to the granule cell layer, where intensely labeled, coarse dendrites were frequently observed at high-power magnification (Figs. 11*B,D,H,* 13*C*).

In the basal dendritic field, reduced staining was observed for all subunits. Immunoreactivity was decreased in seven cases, whereas in the other nine cases, labeling was virtually absent, except for a few stained dendrites, some of which reverted back into the granule cell layer (Figs. 11*B,D,H*, 12, 13*B,C*). These two patterns of reduced immunoreactivity in the subgranular layer were not related to the degree of cell loss in the polymorphic layer. Finally, the most prominent changes were observed in the granule cell layer. Surviving granule cells exhibited increased staining for the α1-, α2-, β2,3-, and γ2-subunits, their somata varying in size and shape (Figs. 11*B,D,* 13*B,C,E*). At the subcellular level, individual granule cells were outlined by intense staining along the surface of the cell bodies (Fig. 13*B,E*) in contrast to discrete staining observed in controls (Fig. 13*A,D*).

In conclusion, alterations in $GABA_A$ receptor subunit immunoreactivity in surviving granule cells show a remarkably polarized pattern with increased staining on the soma membrane and apical dendrites and decreased or no staining in the basal dendritic field. The augmented staining in granule cell and molecular layers suggests an upregulation of receptors in surviving granule cells of TLE patients with HS, despite extensive granule cell loss. The magnitude of changes in staining intensity observed in the granule cells was most obvious for the α2-subunit.

Interneurons immunoreactive for the α1-subunit were mostly conserved in the molecular layer with a preferential localization in the outer part (Fig. 7*C*). Isolated, large and intensely stained cells were also seen, with long dendrites reaching the outer molecular layer and extending into the hilus. Because of loss of staining in the granule cell basal dendrites, the few surviving interneurons were easily identified in the subgranular layer (Fig. 10*H,I*).

Quantitative analysis

Granule cells were counted in Nissl-stained sections adjacent to those used for densitometric measurements. Cell densities in HS specimens were decreased by >50% compared to autopsy and non-HS cases ($p < 0.01$ for both), whereas no difference was found between the autopsy and non-HS groups (Fig. 3*B*). This result was not significantly changed when granule cell numbers were sampled within a 125-μm-wide column to take into account dispersion of granule cell somata (data not shown). Thus, in our HS patient series, granule cell loss was extensive, whereas dispersion was rather limited in most cases.

Differences in $GABA_A$ receptor subunit staining intensity between autopsy, non-HS, and HS groups were assessed quantitatively by densitometry (Fig. 3*D–G*). In the granule cell layer, the HS group showed increased OD for the α1-, α2-, β2,3-, and γ2-subunits, when compared with autopsy specimens (α1- and β2,3-subunits, $p < 0.05$; α2- and γ2-subunits, $p < 0.01$). When compared to non-HS cases, OD was significantly increased for the α2- and β2,3-subunits in the HS group ($p < 0.05$ for both). In the inner and outer molecular layers, increased α2-subunit OD was observed in the HS group when compared to autopsy cases ($p < 0.05$, $p < 0.01$, respectively). In contrast, in the subgranular layer, OD was significantly decreased for all subunits in the HS group when compared either to autopsy specimens (α1-subunit, $p < 0.01$; α2-, α3- and β2,3-subunits, $p < 0.05$) or to non-HS specimens (α1-, α2- and β2,3- subunits, $p < 0.05$; γ2-subunit, $p < 0.01$). In all layers, no significant difference in OD was found for any of the five subunits

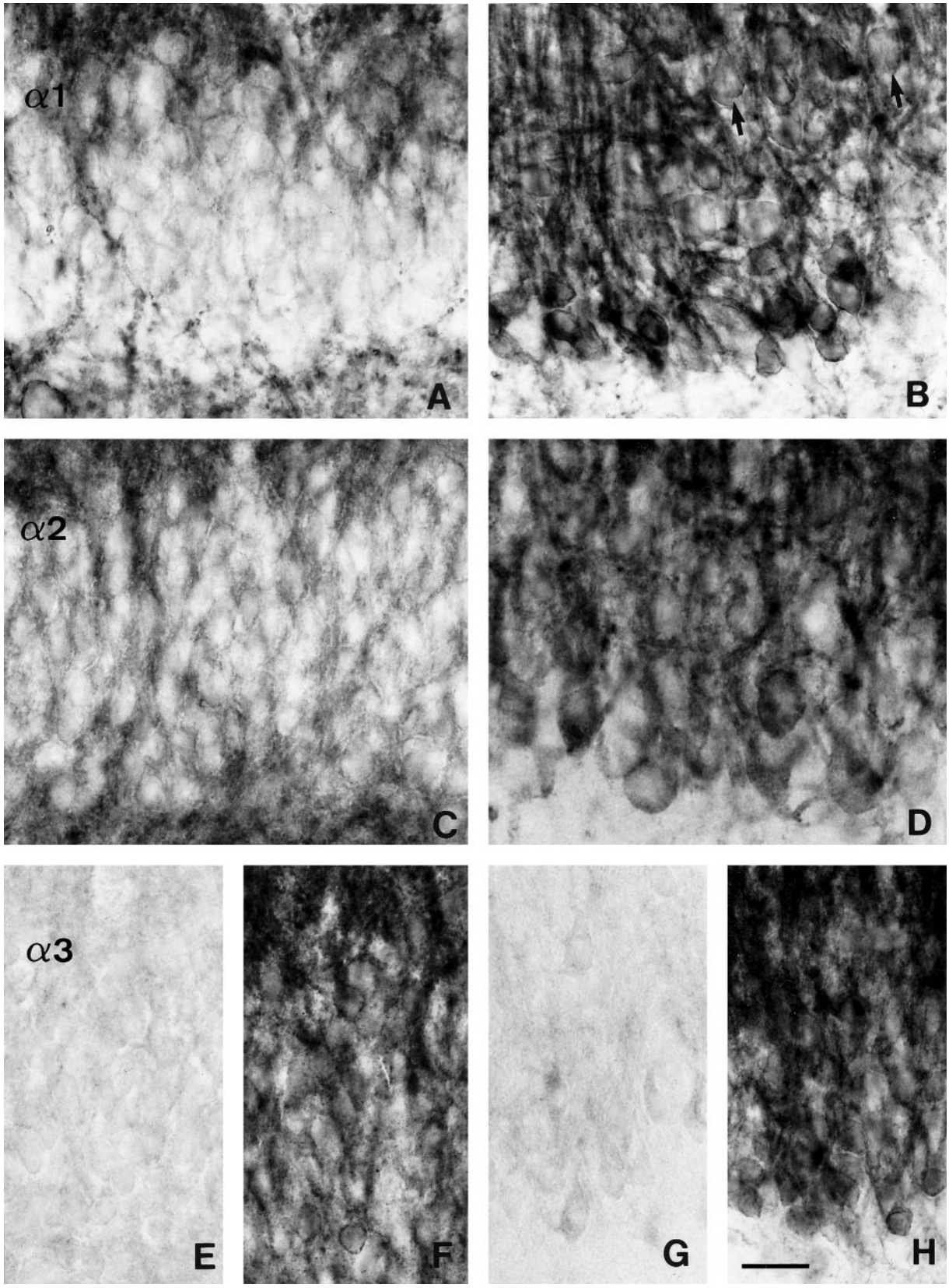

Figure 11. Changes in subunit-specific $GABA_A$ receptor immunoreactivity in the dentate gyrus in TLE with HS (*B, D, G, H*) versus controls (*A, C*, surgery, TLE without HS; *E, F*, autopsy). *A, B,* α1-subunit; *C, D,* α2-subunit; *E–H,* α3-subunit. *A, C,* In control specimens, the somata of granule cells are outlined by faint or no staining for the α1-subunit (*A*) and the α2-subunit (*C*), whereas apical and basal dendritic fields are moderately labeled. *B, D,* In TLE with HS specimens, strongly increased α1-subunit (*B*) and α2-subunit immunoreactivity (*D*) is seen surrounding the somata of granule cells and in the molecular layer, whereas only few basal dendrites remain. Note the granule cell dispersion into the molecular layer in HS (*B, arrows*). *E, F,* Two control specimens illustrate the range of α3-subunit immunoreactivity. Whereas in *E* staining is absent from the granule cells and their dendritic fields, in *F* staining is moderate to intense, outlining the granule cell somata and apical dendrites. *G, H,* In these TLE specimens with HS, α3-subunit immunoreactivity is either absent in dentate gyrus (*G*) or, in *H* shows the same staining pattern as the α1-and α2-subunits. Note the variable size of granule cells. Scale bar, 25 μm.

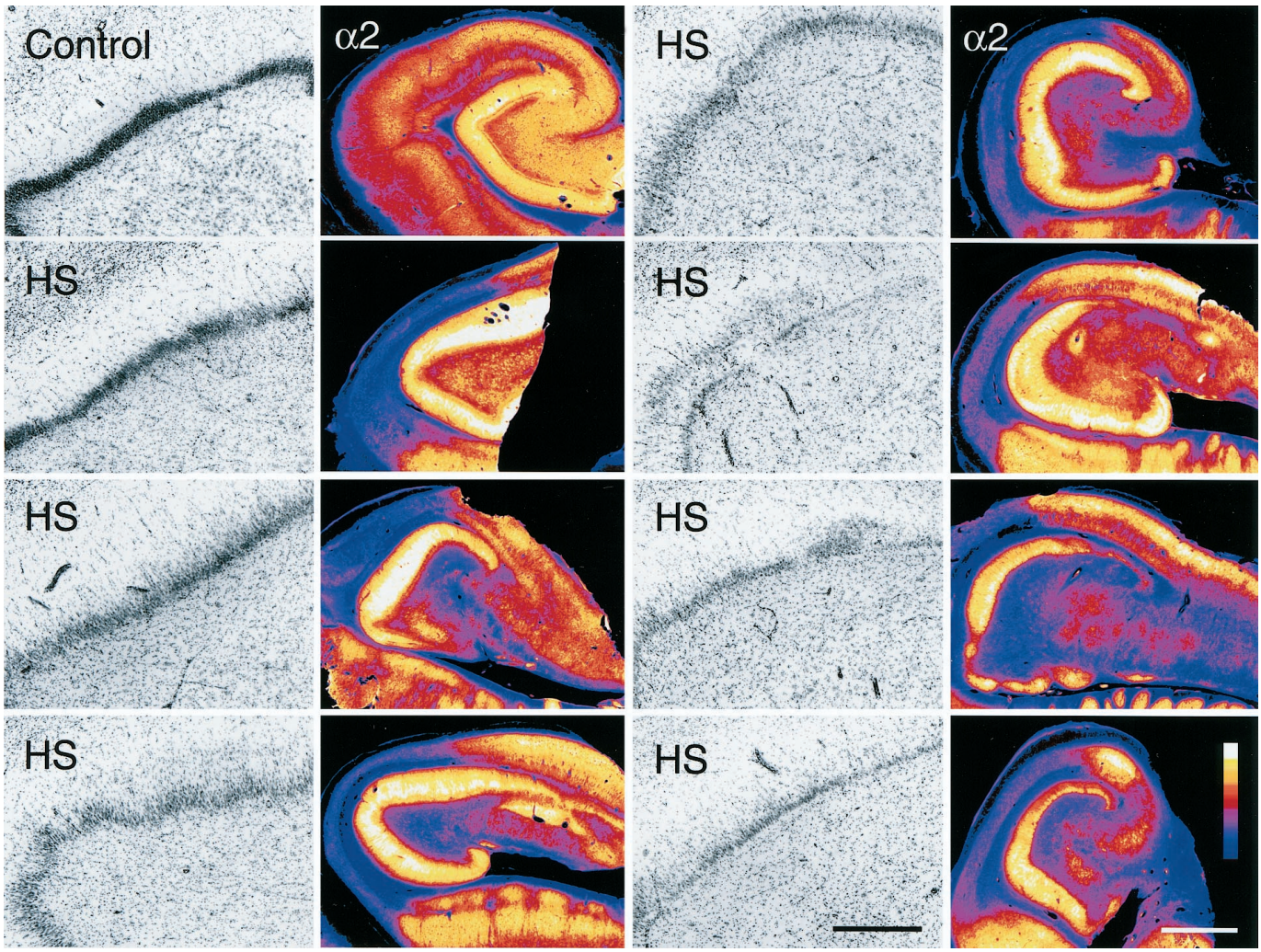

Figure 12. Upregulation of the $GABA_A$ receptor α2-subunit in the dentate gyrus of seven TLE specimens with HS in comparison to a control specimen (autopsy). An overview of the hippocampus is shown in color-coded video images. Adjacent sections stained for Nissl are represented in *black* and *white* at higher magnification, with the upper blade of the dentate gyrus depicted to demonstrate granule cell density. In control hippocampus (*top left panel*), granule cells are tightly packed, forming a compact layer. In HS specimens with moderate granule cell loss, staining intensity in the molecular layer is higher than in controls. In HS specimens with severe granule cell loss, the apparent intensity is similar to that in controls. Scale bars: *Nissl*, 0.5 mm; α2, 2 mm.

between the autopsy group and non-HS cases. Except for a clear decrease in the subgranular layer, α3-subunit OD was not significantly different in the HS group when compared to autopsy and non-HS cases, which reflects the variable degree of granule cell staining for this subunit in all three patient groups, as described above.

DISCUSSION

Two principal conclusions emerge from this study. First, in the normal human hippocampus a differential and neuron-specific expression pattern of $GABA_A$ receptor subtypes was evident, both at the regional and the cellular level. Second, in TLE patients with HS, staining was decreased in areas of prominent cell loss, whereas surviving hippocampal neurons exhibited selective alterations in the expression of the three major $GABA_A$ receptor subtypes. The most striking changes were (1) increased staining for distinct $GABA_A$ receptor subunits on the somata and apical dendrites of granule cells with reduced labeling on the basal dendrites, (2) differential reorganization of the α1-, α2-, and α3-subunits in the CA2 area and in hilar cells, (3) partial and layer-specific loss of α1-subunit-positive interneurons in the hippocampus proper, and (4) altered dendritic morphology in many of the surviving interneurons immunopositive for the α1-subunit.

$GABA_A$ receptor subtype expression in the normal human hippocampus

In previous studies of human hippocampus, only antibodies for the α1- and β2,3-subunits were available to determine $GABA_A$ receptor distribution (Houser et al., 1988; Mizukami et al., 1997, 1998). In addition, expression of the α5-subunit has been shown with ligand binding and autoradiography (Sur et al., 1998; Howell et al., 1999). Using an antigen-retrieval procedure adapted to human brain tissue, specific immunostaining for the α2-, α3-, and γ2-subunits is now also possible (Loup et al., 1998). This has permitted a comprehensive examination of the α1-, α2-, α3-, β2,3-, and γ2-subunits in the present investigation. Based on the staining pattern of the ubiquitously expressed β2,3- and γ2-subunits, we find that the majority of hippocampal $GABA_A$ receptor subtypes appear to be labeled with the antibodies used.

$GABA_A$ receptor heterogeneity in the human hippocampus is best demonstrated with the differential distribution of the α1-, α2-, and α3-subunits, which represent markers of largely distinct receptor subtypes. Thus, whereas all three α-subunits were present in CA1, possibly in the same pyramidal cells, they were differentially expressed in CA2 pyramidal cells, and only the α2-subunit was detected in CA3 pyramidal cells. In the hilus, numerous morphologically distinct cell types were observed, including a population

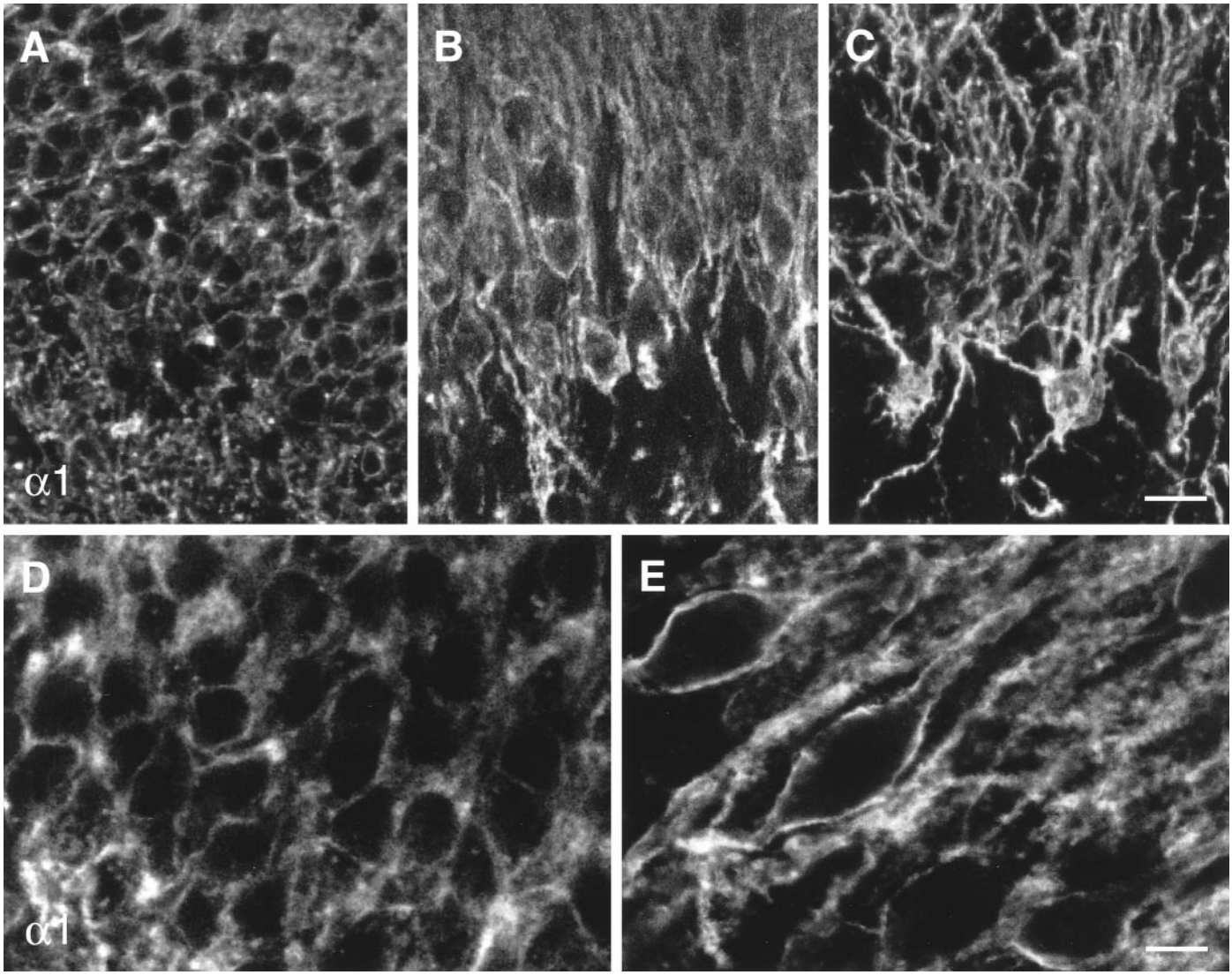

Figure 13. Digital images from confocal laser-scanning microscopy illustrating the increase in $GABA_A$ receptor α1-subunit staining in the dentate granule cell layer in TLE with HS specimens (*B, C, E*) versus controls (*A, D*). In control specimens, discrete α1-subunit immunoreactivity outlines the somata of individual granule cells (*A, D*). In TLE specimens with HS, the surviving granule cells are larger and surrounded by intense staining along the surface of the somata and apical dendrites. Images *A, B, D,* and *E* were each prepared as a stack of four adjacent optical sections at intervals of 0.35 μm (*A, B*) and 0.25 μm (*D, E*), and image *C* is based on the superposition of 30 adjacent optical sections spaced by 0.35 μm. Scale bars: *A–C,* 20 μm; *D, E,* 10 μm.

of α2-subunit-positive pyramidal-like cells located well within the hilar borders. Mossy cells displayed strong staining for both the α1- and the α2-subunits, but not the α3-subunit. Furthermore, many interneurons throughout the hippocampus were positive for the α1-, but not the α2- or α3-subunit.

The strong staining of α1-subunit-positive interneurons revealed a wide variety of cell types in all hippocampal layers and throughout the dentate gyrus. These cells also expressed the β2,3- and γ2-subunits, suggesting the presence of functional $GABA_A$ receptors. According to their morphology and localization, it is likely that these interneurons are a subset of GABA neurons, as reported in human and rodent brain (Gao and Fritschy, 1994; Nusser et al., 1995; Esclapez et al., 1996; Zhang et al., 1998). Compared to rodent, however, a larger diversity in cell types and higher complexity in the distribution of α1-subunit-positive interneurons was observed in the human.

Our results differ in several additional respects from those in rodent brain (Fritschy and Möhler, 1995; Sperk et al., 1997). First, the α3-subunit, which is virtually absent in rodent hippocampus, was strongly expressed in the CA1 area and was present to varying degrees in dentate granule cells. This finding, unique for the α3-subunit in the dentate gyrus, is unlikely to represent an artifact, as the staining intensity for the α3-subunit in CA1, subiculum, and entorhinal cortex was highly comparable between specimens (Loup et al., 1998). Rather, this may reflect a dynamic regulation of this subunit in granule cells. Second, little or no α1-subunit staining was apparent in human CA3 pyramidal cells, whereas moderate α1-subunit immunoreactivity has been reported in rodent CA3 dendritic fields. Third, hilar mossy cells abundantly expressed both the α1- and α2-subunits in human, whereas this has not been observed in rodent. Fourth, prominent staining was observed on the basal dendrites of dentate granule cells. Basal dendrites, which are usually absent in normal rat granule cells, are a common feature in human brain (Seress and Mrzljak, 1987; Lim et al., 1997). These species differences underscore the need for caution in interpreting findings from animal models of human disease.

Altered $GABA_A$ receptor subtype expression in TLE specimens with HS

The following factors must be considered in interpreting our results. First, the age at collection differed between the autopsy subjects and the two surgical patient groups. In agreement with others (Mizukami et al., 1997), we found no evidence of age-related changes in $GABA_A$ receptor subunit immunoreactivity, and cell

numbers appeared to be constant in the autopsy group. Second, the method of procurement did not influence the quality of staining, as shown in Figure 1. Tissue and receptor expression were well preserved, even with postmortem intervals of up to 16 hr (Loup et al., 1998). Third, all surgical TLE patients, with HS and without HS, were receiving antiepileptic treatment and had undergone surgical anesthesia. The strongest finding that argues against therapeutically induced changes accounting for our results is the marked difference in $GABA_A$ receptor expression in HS versus non-HS specimens, even though both were taking similar medication. Furthermore, no differences in expression pattern between autopsy controls and the non-HS group receiving antiepileptic drugs were apparent.

The profound decrease in $GABA_A$ receptor staining in the CA1 and CA3 areas and dentate hilus, where cell loss was most severe, is in agreement with results from other studies (Olsen et al., 1992; Wolf et al., 1994; Koepp et al., 1996; Hand et al., 1997). More importantly, however, the reorganization of $GABA_A$ receptors with maintained or increased levels of intensity in areas of relative cell loss points to an increase in the number of receptors per neuron. This was most apparent for the α2-subunit, indicating a relative increase in $GABA_A$ receptors containing this subunit. The fact that such changes were not recognized in previous investigations may reflect the lower spatial resolution of autoradiography and PET analysis and an unavailability of subunit-specific ligands.

The strongest evidence for an upregulation of $GABA_A$ receptors in individual cells was observed in the dentate gyrus. Similar findings have been obtained in several animal models of TLE (Schwarzer et al., 1997; Brooks-Kayal et al., 1998; Nusser et al., 1998; Bouilleret et al., 2000). Upregulation has been proposed to result from hyperactivity at GABA synapses in dentate granule cells (Schwartzkroin, 1998). This hypothesis is supported by the demonstration of activity-dependent changes in $GABA_A$ receptor expression in animal models of TLE (Brooks-Kayal et al., 1998; Nusser et al., 1998) and observations of reorganized axonal circuits involving GABA neurons in human dentate molecular layer (Babb et al., 1989; de Lanerolle et al., 1989; Mathern et al., 1995b, 1999; Blümcke et al., 1996).

A further interesting finding was the significant reduction in staining in granule cell basal dendrites, even though these are conserved in TLE with HS (Scheibel et al., 1974; Isokawa et al., 1993; von Campe et al., 1997). Thus, there appears to be a redistribution of $GABA_A$ receptors within granule cells with increased expression in apical and decreased expression in basal dendrites. These alterations may be compensatory in response to the recurrent excitation because of mossy fiber sprouting in HS (de Lanerolle et al., 1989; Sutula et al., 1989; Houser et al., 1990; Babb et al., 1991; Zhang and Houser, 1999). Paradoxically, however, the reorganized mossy fibers may ultimately contribute to failure of $GABA_A$ receptor function via a zinc-dependent mechanism (Buhl et al., 1996; Brooks-Kayal et al., 1998; Shumate et al., 1998).

Aberrant mossy fiber innervation has also been described in the CA2 area of TLE patients with HS (Houser et al., 1990; Babb et al., 1992; Williamson and Spencer, 1994). Furthermore, CA2 pyramidal cells in HS appear not to exhibit epileptiform bursts (Williamson and Spencer, 1994). The altered subcellular distribution and expression of the α-subunit variants in CA2 pyramidal cells, which was highly subunit-specific, may represent a structural correlate to this functional finding.

Although substantial hilar cell loss is typical of HS, we show that a number of cell types remained, including mossy cells, which expressed the α1- and α2-subunits, and a subset of interneurons positive for the α1-subunit. Mossy cells were clearly less prevalent than in controls, yet represented a sizable proportion of the surviving neurons labeled for both subunits, indicating that not all are similarly vulnerable to injury. Among α1-subunit-positive interneurons, mostly large multipolar cells were preserved. In dentate hilus, loss of specific subpopulations of GABA neurons (de Lanerolle et al., 1989; Robbins et al., 1991; Mathern et al., 1995b; Maglóczky et al., 2000), as well as preservation of other subclasses (Babb et al., 1989; Sloviter et al., 1991; Mathern et al., 1995b; Blümcke et al., 1996; Maglóczky et al., 2000), have been reported. This highly differentiated sensitivity to seizure-induced damage underscores the functional and neurochemical specialization of inhibitory cells (Freund and Buzsáki, 1996). Furthermore, many of the surviving hilar interneurons exhibited marked changes in dendritic morphology, as reported recently using intracellular dye injections (Blümcke et al., 1999) or immunohistochemical methods (Maglóczky et al., 2000). In our study, moreover, these alterations were also observed in surviving interneurons located in the CA1-CA3 areas. Future quantitative studies will aim at further characterization of dendritic structure.

We observed a massive loss of α1-subunit-positive interneurons in the CA2 and CA3 pyramidal cell layer. Conceivably, these cells might have survived, but no longer express the α1-subunit-containing receptor subtype. This is, however, unlikely on the basis of studies of other neurochemical markers (see above). Laminar loss of a subpopulation of interneurons, which has not been reported before in human or animal models of TLE, suggests that inhibitory drive is altered at specific inputs on surviving neurons in stratum pyramidale.

In conclusion, we have provided the first comprehensive description of the organization of the three major $GABA_A$ receptor subtypes in the human hippocampus. These results reveal a remarkable complexity in $GABA_A$ receptor subunit expression, which may be necessary to fulfill specific functional requirements of distinct inhibitory neuronal circuits. Furthermore, our analysis of hippocampal specimens from TLE patients with HS shows marked changes in $GABA_A$ receptors with reorganization of specific receptor subtypes in surviving principal cells and interneurons. These findings, unique to the human brain, will be of importance in the design of novel diagnostic and therapeutic strategies.

REFERENCES

al-Hussain S, al-Ali S (1995) A Golgi study of cell types in the dentate gyrus of the adult human brain. Cell Mol Neurobiol 15:207–220.

Amaral DG (1978) A Golgi study of cell types in the hilar region of the hippocampus in the rat. J Comp Neurol 182:851–914.

Amaral DG, Insausti R (1990) Hippocampal formation. In: The human nervous system (Paxinos G, ed), pp 711–754. Boston: Academic.

Babb TL, Brown WJ, Pretorius J, Davenport C, Lieb JP, Crandall PH (1984) Temporal lobe volumetric cell densities in temporal lobe epilepsy. Epilepsia 25:729–740.

Babb TL, Pretorius JK, Kupfer WR, Crandall PH (1989) Glutamate decarboxylase-immunoreactive neurons are preserved in human epileptic hippocampus. J Neurosci 9:2562–2574.

Babb TL, Kupfer WR, Pretorius JK, Crandall PH, Levesque MF (1991) Synaptic reorganization by mossy fibers in human epileptic fascia dentata. Neuroscience 42:351–363.

Babb TL, Pretorius JK, Kupfer WR, Mathern GW, Crandall PH, Levesque MF (1992) Aberrant synaptic reorganization in human epileptic hippocampus: evidence for feedforward excitation. Dendron 1:7–25.

Barnard EA, Skolnick P, Olsen RW, Möhler H, Sieghart W, Biggio G, Braestrup C, Bateson AN, Langer SZ (1998) International union of pharmacology. XV. Subtypes of γ-aminobutyric $acid_A$ receptors: classification on the basis of subunit structure and receptor function. Pharmacol Rev 50:291–313.

Blümcke I, Beck H, Nitsch R, Eickhoff C, Scheffler B, Celio MR, Schramm J, Elger CE, Wolf HK, Wiestler OD (1996) Preservation of calretinin-immunoreactive neurons in the hippocampus of epilepsy patients with Ammon's horn sclerosis. J Neuropathol Exp Neurol 55:329–341.

Blümcke I, Zuschratter W, Schewe JC, Suter B, Lie AA, Riederer BM, Meyer B, Schramm J, Elger CE, Wiestler OD (1999) Cellular pathology of hilar neurons in Ammon's horn sclerosis. J Comp Neurol 414:437–453.

Bouilleret V, Loup F, Kiener T, Marescaux C, Fritschy JM (2000) Early loss of interneurons and delayed subunit-specific changes in $GABA_A$-receptor expression in a mouse model of mesial temporal lobe epilepsy. Hippocampus 10:305–324.

Braak H (1974) On the structure of the human archicortex. I The cornu ammonis. A Golgi and pigmentarchitectonic study. Cell Tissue Res 152:349–383.

Brooks-Kayal AR, Shumate MD, Jin H, Rikhter TY, Coulter DA (1998) Selective changes in single cell $GABA_A$ receptor subunit expression and function in temporal lobe epilepsy. Nat Med 4:1166–1172.

Brooks-Kayal AR, Shumate MD, Jin H, Lin DD, Rikhter TY, Holloway KL, Coulter DA (1999) Human neuronal γ-aminobutyric $acid_A$ receptors: coordinated subunit mRNA expression and functional correlates in individual dentate granule cells. J Neurosci 19:8312–8318.

Buhl EH, Otis TS, Mody I (1996) Zinc-induced collapse of augmented

inhibition by GABA in a temporal lobe epilepsy model. Science 271:369–373.
Burdette DE, Sakurai SY, Henry TR, Ross DA, Pennell PB, Frey KA, Sackellares JC, Albin RL (1995) Temporal lobe central benzodiazepine binding in unilateral mesial temporal lobe epilepsy. Neurology 45:934–941.
de Lanerolle NC, Kim JH, Robbins RJ, Spencer DD (1989) Hippocampal interneuron loss and plasticity in human temporal lobe epilepsy. Brain Res 495:387–395.
Engel Jr J (1987) Outcome with respect to epileptic seizures. In: Surgical treatment of the epilepsies (Engel Jr J, ed), pp 553–572. New York: Raven.
Engel Jr J (1998) Etiology as a risk factor for medically refractory epilepsy: a case for early surgical intervention. Neurology 51:1243–1244.
Esclapez M, Chang DK, Houser CR (1996) Subpopulations of GABA neurons in the dentate gyrus express high levels of the α1 subunit of the $GABA_A$ receptor. Hippocampus 6:225–238.
Ewert M, Shivers BD, Luddens H, Möhler H, Seeburg PH (1990) Subunit selectivity and epitope characterization of mAbs directed against the $GABA_A$/benzodiazepine receptor. J Cell Biol 110:2043–2048.
Faull RL, Villiger JW (1988) Benzodiazepine receptors in the human hippocampal formation: a pharmacological and quantitative autoradiographic study. Neuroscience 26:783–790.
Franck JE, Pokorny J, Kunkel DD, Schwartzkroin PA (1995) Physiologic and morphologic characteristics of granule cell circuitry in human epileptic hippocampus. Epilepsia 36:543–558.
Freund TF, Buzsáki G (1996) Interneurons of the hippocampus. Hippocampus 6:347–470.
Fritschy JM, Möhler H (1995) $GABA_A$-receptor heterogeneity in the adult rat brain: differential regional and cellular distribution of seven major subunits. J Comp Neurol 359:154–194.
Fritschy JM, Weinmann O, Wenzel A, Benke D (1998) Synapse-specific localization of NMDA and $GABA_A$ receptor subunits revealed by antigen-retrieval immunohistochemistry. J Comp Neurol 390:194–210.
Gao B, Fritschy JM (1994) Selective allocation of $GABA_A$ receptors containing the α1 subunit to neurochemically distinct subpopulations of rat hippocampal interneurons. Eur J Neurosci 6:837–853.
Hand KS, Baird VH, Van Paesschen W, Koepp MJ, Revesz T, Thom M, Harkness WF, Duncan JS, Bowery NG (1997) Central benzodiazepine receptor autoradiography in hippocampal sclerosis. Br J Pharmacol 122:358–364.
Houser CR (1990) Granule cell dispersion in the dentate gyrus of humans with temporal lobe epilepsy. Brain Res 535:195–204.
Houser CR, Olsen RW, Richards JG, Möhler H (1988) Immunohistochemical localization of benzodiazepine/$GABA_A$ receptors in the human hippocampal formation. J Neurosci 8:1370–1383.
Houser CR, Miyashiro JE, Swartz BE, Walsh GO, Rich JR, Delgado-Escueta AV (1990) Altered patterns of dynorphin immunoreactivity suggest mossy fiber reorganization in human hippocampal epilepsy. J Neurosci 10:267–282.
Howell O, Atack J, McKernan R, Sur C (1999) Mapping of the α5 subunit containing $GABA_A$ receptor in the human hippocampus. Br J Pharmacol 128:292.P.
Hsu SM, Raine L, Fanger H (1981) Use of avidin-biotin-peroxidase complex (ABC) in immunoperoxidase techniques: a comparison between ABC and unlabeled antibody (PAP) procedures. J Histochem Cytochem 29:577–580.
Isokawa M (1996) Decrement of $GABA_A$ receptor-mediated inhibitory postsynaptic currents in dentate granule cells in epileptic hippocampus. J Neurophysiol 75:1901–1908.
Isokawa M, Levesque MF, Babb TL, Engel Jr J (1993) Single mossy fiber axonal systems of human dentate granule cells studied in hippocampal slices from patients with temporal lobe epilepsy. J Neurosci 13:1511–1522.
Johnson EW, de Lanerolle NC, Kim JH, Sundaresan S, Spencer DD, Mattson RH, Zoghbi SS, Baldwin RM, Hoffer PB, Seibyl JP, Innis RB (1992) "Central" and "peripheral" benzodiazepine receptors: opposite changes in human epileptogenic tissue. Neurology 42:811–815.
Kim JH, Guimaraes PO, Shen MY, Masukawa LM, Spencer DD (1990) Hippocampal neuronal density in temporal lobe epilepsy with and without gliomas. Acta Neuropathol 80:41–5.
Koepp MJ, Richardson MP, Brooks DJ, Poline JB, Van Paesschen W, Friston KJ, Duncan JS (1996) Cerebral benzodiazepine receptors in hippocampal sclerosis. An objective *in vivo* analysis. Brain 119:1677–1687.
Koepp MJ, Hand KS, Labbé C, Richardson MP, Van Paesschen W, Baird VH, Cunningham VJ, Bowery NG, Brooks DJ, Duncan JS (1998) In vivo [^{11}C]flumazenil-PET correlates with ex vivo [^{3}H]flumazenil autoradiography in hippocampal sclerosis. Ann Neurol 43:618–626.
Lim C, Blume HW, Madsen JR, Saper CB (1997) Connections of the hippocampal formation in humans. I. The mossy fiber pathway. J Comp Neurol 385:325–351.
Lorente de Nó R (1934) Studies on the structure of the cerebral cortex. II Continuation of the study of the ammonic system. J Psychol Neurol 46:113–177.
Loup F, Wieser HG, Yonekawa Y, Möhler H, Fritschy JM (1997) Subtype-specific upregulation of $GABA_A$-receptors in the hippocampal formation of temporal lobe epilepsy patients. Soc Neurosci Abstr 23:816.
Loup F, Weinmann O, Yonekawa Y, Aguzzi A, Wieser HG, Fritschy JM (1998) A highly sensitive immunofluorescence procedure for analyzing the subcellular distribution of $GABA_A$ receptor subunits in the human brain. J Histochem Cytochem 46:1129–1139.
Loup F, Wieser HG, Aguzzi A, Yonekawa Y, Fritschy JM (1999) Reorganization of $GABA_A$-receptor subtype expression in the CA2 area of the hippocampus in human temporal lobe epilepsy. Soc Neurosci Abstr 25:603.
Maglóczky Z, Wittner L, Borhegyi Z, Halász P, Vajda J, Czirják S, Freund TF (2000) Changes in the distribution and connectivity of interneurons in the epileptic human dentate gyrus. Neuroscience 96:7–25.
Mathern GW, Pretorius JK, Babb TL (1995a) Influence of the type of initial precipitating injury and at what age it occurs on course and outcome in patients with temporal lobe seizures. J Neurosurg 82:220–227.
Mathern GW, Babb TL, Pretorius JK, Leite JP (1995b) Reactive synaptogenesis and neuron densities for neuropeptide Y, somatostatin, and glutamate decarboxylase immunoreactivity in the epileptogenic human fascia dentata. J Neurosci 15:3990–4004.
Mathern GW, Mendoza D, Lozada A, Pretorius JK, Dehnes Y, Danbolt NC, Nelson N, Leite JP, Chimelli L, Born DE, Sakamoto AC, Assirati JA, Fried I, Peacock WJ, Ojemann GA, Adelson PD (1999) Hippocampal GABA and glutamate transporter immunoreactivity in patients with temporal lobe epilepsy. Neurology 52:453–472.
McKernan RM, Whiting PJ (1996) Which $GABA_A$-receptor subtypes really occur in the brain? Trends Neurosci 19:139–143.
Mizukami K, Ikonomovic MD, Grayson DR, Rubin RT, Warde D, Sheffield R, Hamilton RL, Davies P, Armstrong DM (1997) Immunohistochemical study of $GABA_A$ receptor β2/3 subunits in the hippocampal formation of aged brains with Alzheimer-related neuropathologic changes. Exp Neurol 147:333–345.
Mizukami K, Ikonomovic MD, Grayson DR, Sheffield R, Armstrong DM (1998) Immunohistochemical study of $GABA_A$ receptor α1 subunit in the hippocampal formation of aged brains with Alzheimer-related neuropathologic changes. Brain Res 799:148–155.
Möhler H, Fritschy JM, Lüscher B, Rudolph U, Benson J, Benke D (1996) The $GABA_A$ receptors. From subunits to diverse functions. Ion Channels 4:89–113.
Nusser Z, Roberts JD, Baude A, Richards JG, Sieghart W, Somogyi P (1995) Immunocytochemical localization of the α1 and β2/3 subunits of the $GABA_A$ receptor in relation to specific GABAergic synapses in the dentate gyrus. Eur J Neurosci 7:630–646.
Nusser Z, Hájos N, Somogyi P, Mody I (1998) Increased number of synaptic $GABA_A$ receptors underlies potentiation at hippocampal inhibitory synapses. Nature 395:172–177.
Olsen RW, Bureau M, Houser CR, Delgado-Escueta AV, Richards JG, Möhler H (1992) GABA/benzodiazepine receptors in human focal epilepsy. Epilepsy Res [Suppl] 8:383–391.
Olsen RW, DeLorey TM, Gordey M, Kang MH (1999) GABA receptor function and epilepsy. Adv Neurol 79:499–510.
Robbins RJ, Brines ML, Kim JH, Adrian T, de Lanerolle N, Welsh S, Spencer DD (1991) A selective loss of somatostatin in the hippocampus of patients with temporal lobe epilepsy. Ann Neurol 29:325–332.
Scheibel ME, Crandall PH, Scheibel AB (1974) The hippocampal-dentate complex in temporal lobe epilepsy. A Golgi study. Epilepsia 15:55–80.
Schoch P, Richards JG, Häring P, Takacs B, Stähli C, Staehelin T, Haefely W, Möhler H (1985) Co-localization of $GABA_A$ receptors and benzodiazepine receptors in the brain shown by monoclonal antibodies. Nature 314:168–171.
Schwartzkroin PA (1998) GABA synapses enter the molecular big time. Nat Med 4:1115–1116.
Schwarzer C, Tsunashima K, Wanzenböck C, Fuchs K, Sieghart W, Sperk G (1997) $GABA_A$ receptor subunits in the rat hippocampus II: altered distribution in kainic acid-induced temporal lobe epilepsy. Neuroscience 80:1001–1017.
Semah F, Picot MC, Adam C, Broglin D, Arzimanoglou A, Bazin B, Cavalcanti D, Baulac M (1998) Is the underlying cause of epilepsy a major prognostic factor for recurrence? Neurology 51:1256–1262.
Seress L, Mrzljak L (1987) Basal dendrites of granule cells are normal features of the fetal and adult dentate gyrus of both monkey and human hippocampal formations. Brain Res 405:169–174.
Shumate MD, Lin DD, Gibbs JW III, Holloway KL, Coulter DA (1998) $GABA_A$ receptor function in epileptic human dentate granule cells: comparison to epileptic and control rat. Epilepsy Res 32:114–128.
Sloviter RS, Sollas AL, Barbaro NM, Laxer KD (1991) Calcium-binding protein (calbindin-D28K) and parvalbumin immunocytochemistry in the normal and epileptic human hippocampus. J Comp Neurol 308:381–396.
Somogyi P, Takagi H (1982) A note on the use of picric acid-paraformaldehyde-glutaraldehyde fixative for correlated light and electron microscopic immunocytochemistry. Neuroscience 7:1779–1783.
Sperk G, Schwarzer C, Tsunashima K, Fuchs K, Sieghart W (1997) $GABA_A$ receptor subunits in the rat hippocampus I: immunocytochemical distribution of 13 subunits. Neuroscience 80:987–1000.
Sur C, Quirk K, Dewar D, Atack J, McKernan R (1998) Rat and human

hippocampal α5 subunit-containing γ-aminobutyric $acid_A$ receptors have α5β3γ2 pharmacological characteristics. Mol Pharmacol 54:928–933.
Sutula T, Cascino G, Cavazos J, Parada I, Ramirez L (1989) Mossy fiber synaptic reorganization in the epileptic human temporal lobe. Ann Neurol 26:321–330.
von Campe G, Spencer DD, de Lanerolle NC (1997) Morphology of dentate granule cells in the human epileptogenic hippocampus. Hippocampus 7:472–88.
Waldvogel HJ, Kubota Y, Fritschy JM, Möhler H, Faull RL (1999) Regional and cellular localisation of $GABA_A$ receptor subunits in the human basal ganglia: An autoradiographic and immunohistochemical study. J Comp Neurol 415:313–40.
Whiting PJ, Bonnert TP, McKernan RM, Farrar S, Le Bourdellès B, Heavens RP, Smith DW, Hewson L, Rigby MR, Sirinathsinghji DJ, Thompson SA, Wafford KA (1999) Molecular and functional diversity of the expanding GABA-A receptor gene family. Ann NY Acad Sci 868:645–653.
Wieser HG, Yasargil MG (1982) Selective amygdalohippocampectomy as a surgical treatment of mesiobasal limbic epilepsy. Surg Neurol 17:445–457.
Wieser HG, Engel Jr J, Williamson PD, Babb TL, Gloor P (1993) Surgically remediable temporal lobe syndromes. In: Surgical treatment of the epilepsies, Ed 2 (Engel Jr J, ed), pp 49–63. New York: Raven.
Williamson A, Spencer DD (1994) Electrophysiological characterization of CA2 pyramidal cells from epileptic humans. Hippocampus 4:226–237.
Williamson A, Telfeian AE, Spencer DD (1995) Prolonged GABA responses in dentate granule cells in slices isolated from patients with temporal lobe sclerosis. J Neurophysiol 74:378–387.
Williamson A, Patrylo PR, Spencer DD (1999) Decrease in inhibition in dentate granule cells from patients with medial temporal lobe epilepsy. Ann Neurol 45:92–99.
Wolf HK, Spänle M, Müller MB, Elger CE, Schramm J, Wiestler OD (1994) Hippocampal loss of the $GABA_A$ receptor α1 subunit in patients with chronic pharmacoresistant epilepsies. Acta Neuropathol 88:313–319.
Zhang N, Houser CR (1999) Ultrastructural localization of dynorphin in the dentate gyrus in human temporal lobe epilepsy: a study of reorganized mossy fiber synapses. J Comp Neurol 405:472–490.
Zhang N, Tahtakran SA, Houser CR (1998) Interneurons in CA1 of the human hippocampus as revealed by immunohistochemical localization of a neuronal nuclear protein and GABA. Soc Neurosci Abstr 24:716.